J Physiol 600.22 (2022) pp 4939–4961

The Journal of Physiology

The vital role of arcuate nociceptin/orphanin FQ neurones in mounting an oestradiol-dependent adaptive response to negative energy balance via inhibition of nearby proopiomelanocortin neurones

Sarah Sayers[1], Nikki Le[1], Jennifer Hernandez[1], Veronica Mata-Pacheco[1] and Edward J. Wagner[2]

[1]*Graduate College of Biomedical Sciences, Western University of Health Sciences, Pomona, CA, USA*
[2]*College of Osteopathic Medicine of the Pacific, Western University of Health Sciences, Pomona, CA, USA*

Handling Editors: David Wyllie & Conny Kopp-Scheinpflug

The peer review history is available in the Supporting Information section of this article (https://doi.org/10.1113/JP283378#support-information-section).

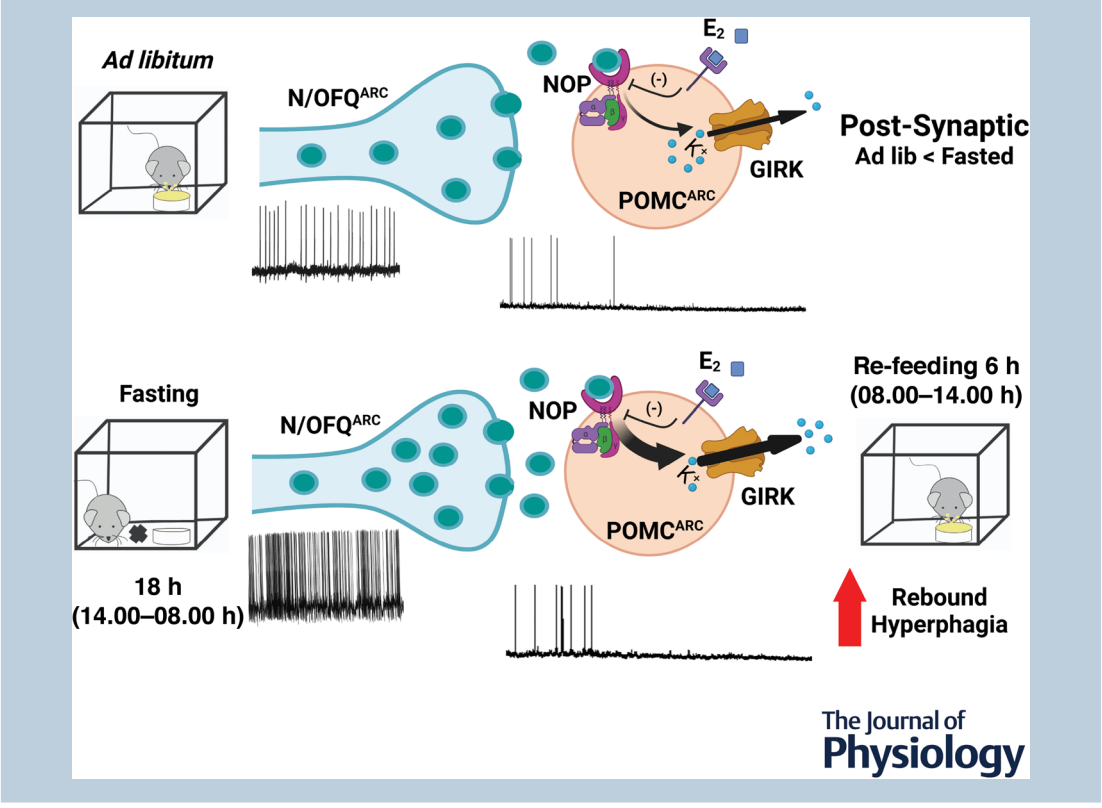

Sarah Sayers obtained her Bachelor of Science degree in Biology from California State University, San Bernardino. She conducted research aimed at determining antiviral targets in the influenza virus utilizing molecular biology techniques as well as investigating the interplay between ageing and Alzheimer's disease in *Drosophila melanogaster*. She received a master's degree in biomedical sciences from Western University of Health Sciences and conducted her thesis research in the laboratory of Dr Edward J. Wagner. This research has garnered her the Florence Haseltine award for best poster presentation by a new investigator at this year's Organization for the Study of Sex Differences conference.

DOI: 10.1113/JP283378

Abstract We tested the hypothesis that N/OFQ neurones in the arcuate nucleus (N/OFQ^{ARC}) inhibit proopiomelanocortin (POMC^{ARC}) neurones in a diet- and hormone-dependent manner to promote a more extensive rebound hyperphagia upon re-feeding following an 18 h fast. We utilized intact male or ovariectomized (OVX) female mice subjected to *ad libitum*-feeding or fasting conditions. N/OFQ^{ARC} neurones under negative energy balance conditions displayed heightened sensitivity as evidenced by a decreased rheobase threshold, increased firing frequency, and increased burst duration and frequency compared to *ad libitum*-feeding conditions. Stimulation of N/OFQ^{ARC} neurones more robustly inhibited POMC^{ARC} neurones under fasting conditions compared to *ad libitum*-feeding conditions. N/OFQ^{ARC} inhibition of POMC^{ARC} neurones is hormone dependent as chemostimulation of N/OFQ^{ARC} neurones from fasted males and OVX females produced a sizable outward current in POMC^{ARC} neurones. Oestradiol (E_2) markedly attenuated the N/OFQ-induced POMC^{ARC} outward current. Additionally, N/OFQ tonically inhibits POMC^{ARC} neurones to a greater degree under fasting conditions than in *ad libitum*-feeding conditions as evidenced by the abrogation of N/OFQ–nociceptin opioid peptide (NOP) receptor signalling and inhibition of N/OFQ release via chemoinhibition of N/OFQ^{ARC} neurones. Intra-arcuate nucleus application of N/OFQ further elevated the hyperphagic response and increased meal size during the 6 h re-feed period, and these effects were mimicked by chemostimulation of N/OFQ^{ARC} neurones *in vivo*. E_2 attenuated the robust N/OFQ-induced rebound hyperphagia seen in vehicle-treated OVX females. These data demonstrate that N/OFQ^{ARC} neurones play a vital role in mitigating the impact of negative energy balance by inhibiting the excitability of anorexigenic neural substrates, an effect that is diminished by E_2 in females.

(Received 27 May 2022; accepted after revision 28 September 2022; first published online 10 October 2022)
Corresponding author E. J. Wagner: Basic Medical Sciences, College of Osteopathic Medicine of the Pacific, Western University of Health Sciences, Director, MSBS Program, 309 E. Second St., Pomona, CA 91766, USA. Email: ewagner@westernu.edu

Abstract figure legend Negative energy balance enhances the excitability of orexigenic N/OFQ^{ARC} neurones relative to that seen in sated, *ad libitum*-fed animals. This leads to heightened inhibitory tone onto anorexigenic proopiomelanocortin (POMC) neurones via increased nociceptin opioid peptide (NOP) receptor-mediated activation of GIRK channels. This in turn leads to an augmented hyperphagic response upon re-feeding following a prolonged fast that helps to correct the energy balance deficit. The presence of oestradiol (E_2) in females attenuates the inhibitory actions of N/OFQ.

Key points

- Nociceptin/orphanin FQ (N/OFQ) promotes increased energy intake and decreased energy expenditure under conditions of positive energy balance in a sex- and hormone-dependent manner.
- Here it is shown that under conditions of negative energy balance, i.e. fasting, N/OFQ inhibits anorexigenic proopiomelanocortin (POMC) neurones to a greater degree compared to homeostatic conditions due to fasting-induced hyperexcitability of N/OFQ neurones.
- Additionally, N/OFQ promotes a sustained increase in rebound hyperphagia and increase in meal size during the re-feed period following a fast.
- These results promote greater understanding of how energy balance influences the anorexigenic circuitry of the hypothalamus, and aid in understanding the neurophysiological pathways implicated in eating disorders promoting cachexia.

Introduction

N/OFQ is an endogenous opioid heptadecapeptide and is an endogenous agonist ligand to the most recently discovered receptor of the opioid receptor superfamily, nociceptin opioid peptide (NOP) receptor (Meunier, 1997). The NOP receptor is expressed in a multitude of areas in the central nervous system, but of utmost interest, NOP receptor is expressed abundantly in the ventromedial nucleus (VMN), paraventricular nucleus (PVN) and arcuate nucleus (ARC) of the hypothalamus,

and the nucleus of the solitary tract, suggesting a role for N/OFQ in energy homeostasis (Bewick et al., 2005; Bunzow et al., 1994; Sinchak et al., 2006). Additionally, the NOP receptor has been implicated in opening G-protein inwardly rectifying potassium (GIRK) channels and eliciting postsynaptic hyperpolarization of steroidogenic factor (SF-1^{VMN}) and proopiomelanocortin ($POMC^{ARC}$) neurones, thereby preventing propagation of action potentials (Borgquist et al., 2013; Chee et al., 2011; Conde et al., 2016; Hernandez et al., 2019; Wagner et al., 1998).

I.C.V. administration of N/OFQ elicits orexigenic effects and decreases core body temperature, effects that are analogous to those evoked by neuropeptide Y (NPY) (NPY; Kotz et al., 1998; Matsushita et al., 2009; Polidori et al., 2000; Pomonis et al., 1996; Stratford et al., 1997). The orexigenic effects of N/OFQ have been delimited to the hypothalamus following a study of I.C.V. administration of N/OFQ to the third ventricle inducing a hyperphagic response in mice fed chow or moderately high fat diet. Additionally, a rise in fat mass, plasma leptin, insulin and cholesterol was observed. Focal injection of N/OFQ into the ARC promoted energy intake and hyperphagia (Hernandez et al., 2019, 2021). Ultimately, central administration of N/OFQ induced an increase in food intake and body weight in mice, and the N/OFQ-induced alterations of these parameters were potentiated under high fat diet (HFD) conditions (Hernandez et al., 2019; Matsushita et al., 2009). N/OFQ induces orexigenic effects in large part via inhibition of $POMC^{ARC}$ neurones, thereby inhibiting the anorexigenic circuitry (Hernandez et al., 2019).

N/OFQ also acts presynaptically to reduce the amount of glutamate released onto its postsynaptic target. Bath application of N/OFQ decreases glutamatergic excitatory postsynaptic currents (EPSCs) in the rat amygdala and ARC (Emmerson & Miller, 1999; Meis & Pape, 2001). In the latter region among the main downstream recipients of this glutamatergic input are the $POMC^{ARC}$ neurones, and they receive this input from SF-1^{VMN} neurones (Conde et al., 2017; Fabelo et al., 2018). N/OFQ reduces the amplitude of electrically and optogenetically evoked EPSCs in POMC neurones, and this inhibitory effect is potentiated under conditions of diet-induced obesity (DIO) (Farhang et al., 2010; Hernandez et al., 2019). This heightened sensitivity to the NOP receptor-mediated inhibition of glutamate release at SF-1^{VMN}/$POMC^{ARC}$ synapses results in more robust hyperphagia and decrease in energy expenditure when N/OFQ is administered into the ARC of DIO mice (Hernandez et al., 2019).

In addition to the orexigenic effects induced by N/OFQ being dependent on energy status, sexual differences also come into play. Males are more responsive to the pleiotropic effects of N/OFQ compared to cycling females. Pro-oestrus (where oestradiol (E_2) levels are highest) and dioestrus (where E_2 sensitivity is highest) females exhibit dampened effects of N/OFQ on homeostatic and hedonic feeding compared to their male counterparts due to the presence of E_2 (Andrews et al., 1981; Gallo & Bona-Gallo, 1985; Hernandez et al., 2019, 2021). E_2 attenuates the N/OFQ-induced activation of GIRK channels in $POMC^{ARC}$ and SF-1^{VMN} neurones (Borgquist et al., 2013, 2014; Conde et al., 2016; Hernandez et al., 2019, 2021). E_2 also diminishes the NOP receptor-mediated presynaptic inhibition of glutamatergic input onto $POMC^{ARC}$ neurones (Borgquist et al., 2013, 2014). This attenuation of the pleiotropic actions of N/OFQ on POMC neurones is abrogated in E_2-primed, progesterone-treated ovariectomized (OVX) females, as the sensitivity to the pre- and postsynaptic effects of N/OFQ exerted in these cells was restored (Borgquist et al., 2014). The actions of E_2 binding to oestrogen receptor α (ERα) or the Gq-membrane oestrogen receptor (Gq-mER) in POMC neurones leads to activation of a phospholipase C (PLC), phosphatidylinositol-3-kinase (PI3K), protein kinase C (PKC), protein kinase A (PKA) and neuronal nitric oxide synthase (nNOS) signal cascade as was evidenced by bath application of N/OFQ in the presence or absence of E_2 during electrophysiological recordings in slices from OVX females. Inhibition of PLC, PI3K, PKC or PKA during electrophysiological experiments blocked the E_2-induced attenuation of NOP-mediated activation of GIRK currents elicited by N/OFQ, whereas pharmacological activation of these signalling molecules mimicked the effect of E_2 (Conde et al., 2016). This signalling cascade disrupts $G_{i/o}$-coupled receptors from activating GIRK channels, notably in $POMC^{ARC}$ neurones (Kelly & Wagner, 1999; Qiu et al., 2006).

With growing rates of eating disorders ranging from anorexia nervosa to obesity (Saper et al., 2002; Zigman & Elmquist, 2003), as well as diseases such as HIV/AIDS and cancer, which are associated with increased energy expenditure resulting in wasting and cachexia (Inui, 2002; Riggs et al., 2012), it is important to understand the pathoneurogenic mechanisms underlying the alterations in food intake and energy expenditure observed in these opposing states. Ample evidence collected over the past 25 years demonstrates that exogenous N/OFQ induces sex- and energy status-dependent inhibition of $POMC^{ARC}$ neurones and accompanying hyperphagia. More recent findings indicate N/OFQ^{ARC} neurones can similarly inhibit $POMC^{ARC}$ neurones upon optogenetic stimulation through a combination of NOP receptor-mediated activation of GIRK channels and fast $GABA_A$ receptor-mediated neurotransmission to drive homeostatic feeding (Hernandez et al., 2021; Jais et al., 2020). These N/OFQ^{ARC} neurones are inhibited by leptin and glucose, and their excitability is heightened upon HFD feeding (Jais et al., 2020). This project sought to examine the other end of the energy balance spectrum, namely fasting. Therefore, our working hypothesis is

that the excitability of N/OFQ^{ARC} neurones and the associated inhibitory tone onto POMC^{ARC} neurones is significantly enhanced under conditions of negative energy balance, which leads to a pronounced hyperphagia upon reintroduction of food following a prolonged fast. We further posit that the fasting-induced alterations in N/OFQ^{ARC} neuronal excitability, inhibition of POMC^{ARC} neurones and rebound hyperphagia occurs in a sexually dimorphic manner and is attenuated by E_2 in OVX females. Using a strategic combination of brain slice electrophysiology and behaviour, we generated data collectively demonstrating that N/OFQ^{ARC} neurones play a pivotal role in promoting a rebound hyperphagic response under conditions of negative energy balance via inhibition of anorexigenic POMC neurones.

Methods

Ethical approval

The entirety of animal care and procedures were compliant with the NIH *Guide for the Care and Use of Laboratory Animals* and approved by Western University of Health Sciences' Institutional Animal Care and Use Committee. Adult male and female prepronociceptin (PNOC)-*cre* mice bred on a C57BL/6 background were obtained from Dr Michael Brucas at the University of Washington and bred in-house. Enhanced green fluorescent protein (eGFP) POMC mice were purchased from The Jackson Laboratory (Bar Harbor, ME, USA; stock no. 009593; C57BL/6 background) and bred in-house. PNOC-*cre*/eGFP-POMC double transgenic mice were generated in-house via breeding of hemizygous PNOC-*cre* mice with hemizygous eGFP-POMC mice. Animals maintained a 12:12 h light–dark cycle (lights on: 06.00–18.00 h), at a constant temperature of 25°C. Food and water were provided *ad libitum* until random assignment to one of two chow access conditions (*ad libitum*-fed *versus* fasted). In-house litters received ear snips upon weaning at 21 days of age, which were then subject to standard polymerase chain reaction (PCR) techniques to detect presence of *cre* and/or eGFP amplicons. Animals used for experimentation ranged from 15 to 26 g in weight and 91 to 122 days of age.

Fasting protocol

PNOC-*cre*, eGFP-POMC and double transgenic PNOC-*cre*/eGFP-POMC mice were randomly assigned to either *ad libitum* feeding or fasting conditions. Animals assigned to the fasting cohort were subject to an 18-h fast between feedings. All animals maintained a standard chow (Teklad Rodent Diet, Teklad Diets, Madison, WI, USA), which provided 18% of calories from fat, 24% from protein and 58% from carbohydrates. Standard chow was available for 6 h (08.00–14.00 h) for the fasting cohort for five consecutive days. Water was available *ad libitum* for all animals.

Surgical procedures

For all experiments female PNOC-*cre*, eGFP POMC, double transgenic PNOC-*cre*/eGFP-POMC and wild-type (WT) mice were ovariectomized 5 days before experimentation under 2% isoflurane anaesthesia. Anaesthetized animals were administered carprofen (0.2 mg/kg; s.c.) to mitigate pain throughout the procedure. They were then placed on their side on a sterile, surgical drape on top of a water-circulating heating pad to prevent hypothermia. The incision site was located approximately 0.5 cm posteriorly from the 12th floating rib. A scalpel was used to create a 0.5 cm incision at a 45-degree angle. Following incision, light irrigation with three to five drops of local anaesthetic (0.5% bupivacaine with adrenaline 1:200,000) commenced to minimize intraoperative bleeding and further reduce intraoperative pain. Two vertical nerve bundles running directly under the initial incision site were located and a 1–2 cm incision was made into the muscle wall between the two nerve bundles. Care was taken to cut only the muscle and not any underlying tissues or organs. Following the second incision into the muscle wall, an ovarian fat pad was revealed which, generally, the ovary was found lying under at the juncture of fat and intestines. The edge of the fat pad was lifted and with the use of forceps, the ovarian suspensory ligament was gently grasped and gently lifted to reveal the ovary. The ovarian ligament and blood supplies were clamped with a haemostat, with care to keep the ovary as close to its natural position as possible. The haemostat was never to twist, as any tension or pulling may cause severe haemorrhage. Instead, the haemostat rested on the animal's body to prevent any pulling. The clamped bundle was ligated with a 3-0 or 4-0 Vicryl suture and the ovary was cut away. The tissue was allowed to retract into the body cavity and the muscle wall was closed with absorbable 3-0 Vicryl suture material, and the skin was sutured closed with a 4-0 Vicryl suture.

Adeno-associated viral vector (AAV) constructs were focally injected into the PNOC-*cre* and double transgenic PNOC-*cre*/eGFP-POMC mice. Transgenic mice were placed under 2% isoflurane and fixed onto a stereotaxic frame (Stoelting, Wood Dale, IL, USA). An incision was created to expose the skull, and a hole was drilled either unilaterally or bilaterally at the midsagittal suture to enable the injection needle to be lowered into the ARC (coordinates from bregma: AP, −0.6 mm; ML, ±0.3 mm; DV, −5.9 mm). *Cre* recombinase-dependent AAV vectors containing either cation channel rhodopsin-2 (ChR2; Mattis et al., 2012; AAV1.EF1a.DIO.ChR2 [E123A].YFP.WPRE.jGH; 7.2 ×

10^{12} genomic copies/ml; 300 nl total volume; Addgene (Watertown, MA, USA) plasmid no. 35507), excitatory designer receptor exclusively activated by designer drug (DREADD; pAAV-hSyn-DIO-hM3D(Gq)-mCherry; 7×10^{12} genomic copies/ml; 300 nl total volume; Addgene plasmid gifted by Bryan Roth, no. 44361), inhibitory DREADD (pAAV-hSyn-DIO-hM4D(Gi)-mCherry; 7×10^{12} genomic copies/ml; 300 nl total volume; Addgene plasmid gifted by Bryan Roth, no. 44362), or their respective enhanced yellow fluorescent protein (eYFP; Mattis et al., 2012; pAAV-Ef1a-DIO EYFP; 1.0×10^{13}; 300 nl total volume; Addgene plasmid deposited by Karl Deisseroth, no. 27056) and mCherry blank controls (pAAV-hSyn-DIO-mCherry; 7×10^{12} genomic copies/ml; 300 nl total volume; Addgene plasmid gifted by Bryan Roth, no. 50459) were administered over a span of 2 min to double transgenic PNOC-*cre*/eGFP POMC mice, PNOC-*cre* mice and WT controls. Prior to infusion of the viral construct, the injection needle remained in place for 5 min, and 10 min after infusion to ensure complete diffusion from injector tip. The injection needle was then slowly removed from the brain to ensure localization of virus to the ARC. Animals were used for experimentation 2–3 weeks following injection of viral construct.

In some experiments, a 26-gauge guide cannula (Plastics One, Roanoke, VA, USA) was stereotaxically implanted into the ARC of WT mice in a similar fashion as described above. Anaesthetized animals secured on a stereotaxic frame received an incision in the scalp, and a unilateral hole was drilled in the skull to allow for the guide cannula to be inserted 1 mm above the ARC (AP, −0.6 mm; ML, −0.3 mm; DV, −4.9 mm). C&B Metabond dental cement (Parkell, Edgewood, NY, USA) was utilized to fix the guide cannula in place. Post-surgery, a stylet was inserted into the guide cannula to keep the lumen patent. Experimentation commenced 1 week post-op to allow full recovery. During experimentation, an injector needle was inserted into the ARC (1 mm below the tip of the guide cannula) so that we could administer N/OFQ or its filtered 0.9% saline vehicle directly into this brain region. Only animals for which there was precise targeting of injection and cannula placement were used. After every surgical procedure, triple antibiotic ointment was applied topically to the incision site after closure. Animals were placed in clean home cages with food and water available *ad libitum*. Home cages were placed on top of a heating pad and animals were monitored for 3 days to ensure proper post-operative healing.

Drugs

Drugs were purchased from Tocris Bioscience/R&D Systems (Minneapolis, MN, USA) unless stated otherwise. Electrophysiological experiments utilized Na^+ channel blocker tetrodotoxin (TTX) prepared as a 1 mM stock solution in UltraPure H_2O. The TTX stock solution was then further diluted with artificial cerebral spinal fluid (aCSF) to a working concentration of 500 nM. The NOP receptor antagonist [$Nphe^1$, Arg^{14}, Lys^{15}]nociceptin-NH_2 (UFP-101) was prepared as a 1 mM stock by dissolving in filtered UltraPure H_2O, and further diluted to a 100 nM working concentration with aCSF. Clozapine-*N*-oxide (CNO) was dissolved in UltraPure H_2O to create a stock concentration of 5 mM, and further diluted with aCSF to a working concentration of 5 μM. E_2 (1,3,5(10)-estratrien-3,17β-diol, 17β-oestradiol; Steraloids, Newport, RI, USA) was dissolved in punctilious ethanol for a stock concentration of 1 mM; the addition of aCSF diluted the stock to a working concentration of 100 nM.

For behavioural experiments, N/OFQ was dissolved in filtered saline and prepared as a 1.5 mM stock solution. N/OFQ was injected directly into the ARC at a concentration of 0.3 nM. Oestradiol benzoate (EB; Steraloids) was prepared as a 1 mg/ml stock solution in punctilious ethanol. A known quantity of this EB stock was added to a volume of sesame oil to produce a final concentration of 20 μg/ml following ethanol evaporation. 11-(1-Piperazinyl)-5*H*-dibenzo[*b*,e][1,4]diazepine (DREADD agonist 21) (Tocris Bioscience) was dissolved in filtered 0.9% saline to a final concentration of 0.3 mg/ml, and delivered systemically in a total volume of 1 ml/kg. All aliquots of stock solutions were stored at 4 or −20°C until experimentation.

Hypothalamic slice preparation

On the day of experimentation, 32% isoflurane was utilized to briefly anaesthetize the animal and rapid decapitation ensued. The brain was quickly and carefully extracted from the skull and dissected to procure the hypothalamic area in the coronal plane. The hypothalamus was then mounted on a cutting platform which was secured in a vibratome filled with an ice-cold, oxygenated (95% O_2, 5% CO_2) sucrose-based cutting solution (in mM: $NaHCO_3$ 26; dextrose 10; HEPES 10; sucrose 208; KCl 2; NaH_2PO_4 1.25; $MgSO_4$ 2, $CaCl_2$ 1). Four to five slices (300 μm in thickness) were obtained through the rostrocaudal extent of the ARC. The ARC slices were then transferred to an auxiliary chamber filled with room temperature oxygenated aCSF (containing the following, in mM: NaCl 62; KCl 2.5; NaH_2PO_4 5.75; HEPES 19.75; dextrose anhydrous 3; $NaHCO_3$ 6; $MgSO_4$ 1; $CaCl_2$ 1), where they incubated until electrophysiological recording.

Electrophysiology

Whole-cell patch clamp electrophysiological recordings from ARC neurones utilizing biocytin-filled electrodes

were performed in hypothalamic slices prepared from intact male and OVX female PNOC-*cre*, eGFP-POMC, and double transgenic PNOC-*cre*/eGFP-POMC mice randomly assigned to *ad libitum* or fasting feeding conditions. During recordings, slices were maintained in a chamber continuously perfusing warmed (35°C), oxygenated aCSF with the $CaCl_2$ concentration raised to 2 mM. The aCSF and all drugs diluted with aCSF were perfused via peristaltic pump at a rate of 1.5 ml/min. Patch electrodes were prepared from borosilicate glass (World Precision Instruments, Sarasota, FL, USA; 1.5 mm OD) pulled on a P-97 Flaming–Brown puller (Sutter Instrument Co., Novato, CA, USA), and filled with internal solution (containing the following, in mM: potassium gluconate 128; NaCl 10; $MgCl_2$ 1; EGTA 11; HEPES 10; ATP 1; GTP 0.25; 0.5% biocytin; adjusted to a pH of 7.3 with KOH; osmolality 286 to 320 mOsm) or, for some experiments, an internal solution (containing the following, in mM: potassium gluconate 128; NaCl 10; $MgCl_2$ 1; BAPTA 8; HEPES 10; ATP 1; GTP 0.25; 0.5% biocytin; adjusted to a pH of 7.3 with KOH; osmolality 286–320 mOsm). Electrode resistances varied from 3 to 8 MΩ.

Recordings were made on an Olympus (Tokyo, Japan) BX51 W1 fixed stage microscopes equipped with infrared differential interference contrast (DIC) video imaging. Multiclamp 700A or 700B preamplifiers (Molecular Devices, LLC, San Jose, CA, USA) served to amplify potentials and pass current through the electrode. Digidata 1550A or 1550B interfaces (Molecular Devices) coupled to pClamp 10.5 or 11.2 software, respectively, were utilized to perform analog to digital conversion of membrane currents and voltages. Access resistance, resting membrane potential (RMP) and input resistance were constantly monitored throughout all recordings. If the access resistance deviated more than 10% from the original value, recording was terminated. Low-pass filtering of currents was conducted at a frequency of 2 kHz. Liquid junction potential was calculated as 10 mV, and corrected for with pClamp software during data analysis. All voltage clamp recordings were performed at a holding potential of −60 mV.

To determine differences in intrinsic activity of PNOC-*cre* neurones in differing energy states (*ad libitum*-fed *versus* fasted), PNOC-*cre*^{ARC} neurones were recorded from ARC slices obtained from PNOC-*cre* animals injected with a *cre*-dependent AAV vector containing eYFP blank construct 2–3 weeks post-experimentation. These recordings were conducted in current clamp, and the membrane potential and firing rate were continuously monitored at rest for 10 min. Rheobase was established as the lowest current (pA) injected to reach membrane threshold and elicit an action potential. Establishing rheobase was achieved by observing the membrane potential in current clamp, and utilization of a current step stimulation protocol where the current was increased by 1–2 pA in a series of 15 steps, for a duration of 150 ms per step. Upon reaching threshold, the amount of current necessary to trigger an action potential was recorded. Basal firing frequency was established in observational current clamp recordings and was calculated as the number of action potentials per second. Plateau potential frequency was determined by the number of burst firing occurrences per second, and further analysed for duration, magnitude and firing frequency. Duration of a plateau potential was determined by the average time in seconds that the membrane remains depolarized measured for each such incident, magnitude was determined by measuring the change in membrane potential from baseline to the depolarized peak of each plateau potential, and firing frequency was measured by the average number of action potentials elicited within each plateau. Each current clamp recording spanned a length of 10 min.

To determine whether fasting altered the ability of ARC N/OFQ neurones to inhibit POMC neurones in a sex-dependent manner, excitatory Gq-coupled DREADD-, inhibitory Gi-coupled DREADD-, or ChR2-injected injected male and OVX female double transgenic PNOC-*cre*/eGFP-POMC mice, both fasted and *ad libitum* cohorts, were utilized 2–3 weeks post-injection into the ARC. mCherry- and eYFP-injected mice were utilized as controls. A baseline current–voltage (*I–V*) relationship from a holding potential of −60 mV was generated by administering pulses (10-mV increments; 150 ms duration) ranging from −50 to −140 mV. For the *in vitro* chemogenetic experiments, following establishment of baseline *I–V* relationship, CNO (5 μM) was bath applied to the ARC slice in the chamber and the membrane current was continuously monitored. Subsequent to establishment of a new steady state, a second *I–V* relationship was acquired. During the CNO washout, membrane current was continuously monitored until the return to the original baseline current was achieved, and a final *I–V* relationship was taken to determine reversibility of CNO-induced effects. For the optogenetic experiments, photostimulation was performed at 20 Hz for 10 s (Chang et al., 2021; Hernandez et al., 2021; Le et al., 2021; Qiu et al., 2016) and the membrane current monitored until a new steady-state level was reached. Similar to the chemogenetic protocol described above, *I–V* relationships were recorded before optogenetic stimulation, after stimulation and following a washout period.

To determine if fasting alters endogenous N/OFQ inhibitory tone in POMC neurones, we first bath applied the high affinity NOP receptor antagonist UFP-101 to ARC slices obtained from male eGFP-POMC mice. We also used a chemogenetic approach during recordings in slices from Gi-coupled DREADD-injected male PNOC-*cre* mice. After obtaining the baseline *I–V*, either

UFP-101 (100 nM) or CNO (5 μM) was added. We then constantly monitored the membrane current until we observed a new steady state value, at which time a second *I–V* relationship was acquired. During drug clearance, membrane current was again continuously monitored until the original baseline was achieved. One last *I–V* relationship was taken to ensure reversibility. Generation of the *I–V* relationships was performed as described above.

Behavioural studies

Behavioural studies were conducted utilizing Comprehensive Lab Animal Monitoring System (CLAMS; Columbus Instruments, Columbus, OH, USA) containing four stations, as previously described and validated (Farhang et al., 2010; Hernandez et al., 2019). Energy intake and meal size were monitored in intact male and OVX female WT and PNOC-*cre* mice. An electronic balance measured the amount of food contained within each food trough and reported the amount consumed by each animal. Each trough was equipped with an outer spillage container to prevent overestimation of the actual amount consumed. Animals were allowed to acclimate in the experimental CLAMS chambers for a 3-day period. In the afternoon, all animals were weighed, handled and returned to their own respective monitoring chambers. Following acclimation, a 5-day monitoring phase was initiated. At 14.00 h on acclimation day 3, animals were removed from their CLAMS chambers and placed into their home cages. Water remained available *ad libitum* and all chow was removed from each cage, which initiated the 18-h fasting period. For cannulated behavioural experiments, the animals were injected directly into the ARC each day at 08.00 h with either N/OFQ (0.3 nM) or its 0.9% saline vehicle (0.2 μl). OVX female WT mice were randomly assigned either EB (20 μg/kg, s.c.) or its sesame oil vehicle (1 ml/kg, s.c.) every other day for the duration of the experiment, beginning at acclimation day 2 to experiment day 5. Fasted mice were placed in CLAM chambers immediately following injection and monitored for the duration of their feeding period (08.00–14.00 h), weighed and placed back into their respective home cages with water available *ad libitum*. Parameters of energy intake and expenditure were continuously written to a computer via an A/D converter to which food intake and energy balance were evaluated. For chemogenetic behavioural experiments utilizing bilaterally injected excitatory or inhibitory DREADDs into the ARC OF PNOC-*cre* or WT male animals, the monitoring and food availability were performed as described above. However, in lieu of intra-ARC injections of N/OFQ or its saline vehicle, animals received subcutaneous injections of either the DREADD agonist Compound 21 (C21; 0.3 mg/kg, s.c.) or its 0.9% saline vehicle (1 ml/kg, s.c.) at 08.00 h.

Immunohistochemistry

Slices from WT and PNOC-*cre* mice were processed for immunohistochemistry to determine c-fos expression in ARC neurones from animals injected 2 h prior with C21. Slices were initially fixed with 4% paraformaldehyde in Sorenson's phosphate buffer (pH 7.4) overnight. They were then immersed for 3 days in 20% sucrose dissolved in Sorensen's buffer, which was changed daily, and frozen in Tissue-Tek embedding medium (Miles, Inc., Elkhart, IN, USA) the next day. Coronal sections (20 μm) were cut on a cryostat and mounted on chilled slides. These sections were then washed with 0.1 M phosphate-buffered saline (PBS; pH 7.4), and then processed overnight with polyclonal antibodies directed against c-fos (Santa Cruz Biotechnology, Dallas, TX, USA; 1:500). This was followed the next day by two 15 min washes with PBS, and then a 2 h incubation with biotinylated goat anti-rabbit secondary antibody (Jackson ImmunoResearch Laboratories, Inc., West Grove, PA, USA; 1:300). After another series of three 15 min PBS washes, there was a final 2 h overlay with streptavidin-Alexa Flour 488 (Thermo Fisher Scientific, Waltham, MA, USA; 1:600), followed by a final series of three 30 min PBS washes and coverslipping the slides. The slides were evaluated using fluorescence immunohistochemistry on a Zeiss Axioskop 2 Plus (Zeiss Microscopy, Jena, Germany). Cell counts taken from an $\sim$0.12 mm^2 area within the dorsomedial VMN were determined in triplicate.

Statistical analysis

Student's *t*-test was utilized to draw comparisons between two groups. Normality was determined *a priori* by verifying skewness and kurtosis were within acceptable limits. For comparisons made between more than two groups, either one-way or repeated-measures, multifactorial analysis of variance (ANOVA) followed by the least significant difference (LSD) test was performed. Comparison of categorical variables was conducted using the chi-square test. Outlier identification was ascertained via Grubb's test. The data are expressed as the mean $\pm$ 1 standard deviation (SD). *n* refers to the number of cells, slices and/or animals. Differences were considered statistically significant if the α probability was <0.05.

Results

N/OFQ neurones exhibit calcium-dependent hyperactivity and decreased rheobase threshold under conditions of negative energy balance

Previous studies depict that N/OFQ induces an inhibitory tone onto $POMC^{ARC}$ neurones, actions that are potentiated under conditions of positive energy

balance (i.e. diet-induced obesity) when compared to lean *ad libitum* chow-fed animals (Hernandez et al., 2019; Hernandez et al., 2021). Taking this into consideration, we deduced that under conditions of negative energy balance (i.e. fasting), N/OFQ^{ARC} neurones would be hyperexcitable. To test this working hypothesis, we observed and quantified the firing patterns of N/OFQ^{ARC} neurones in PNOC-*Cre* mice in both *ad libitum* and fasting conditions. A coronal section highlighting the area of interest is provided in Fig. 1*A*. We used whole-cell patch clamp recordings of N/OFQ^{ARC} neurones that were visualized with eYFP (Fig. 1*B*–*D*), and baseline membrane potential was monitored and recorded for 10 min. Representative traces of N/OFQ^{ARC} neurones recorded from fasted mice displayed increased firing rate and depolarization compared to their *ad libitum*-fed counter-

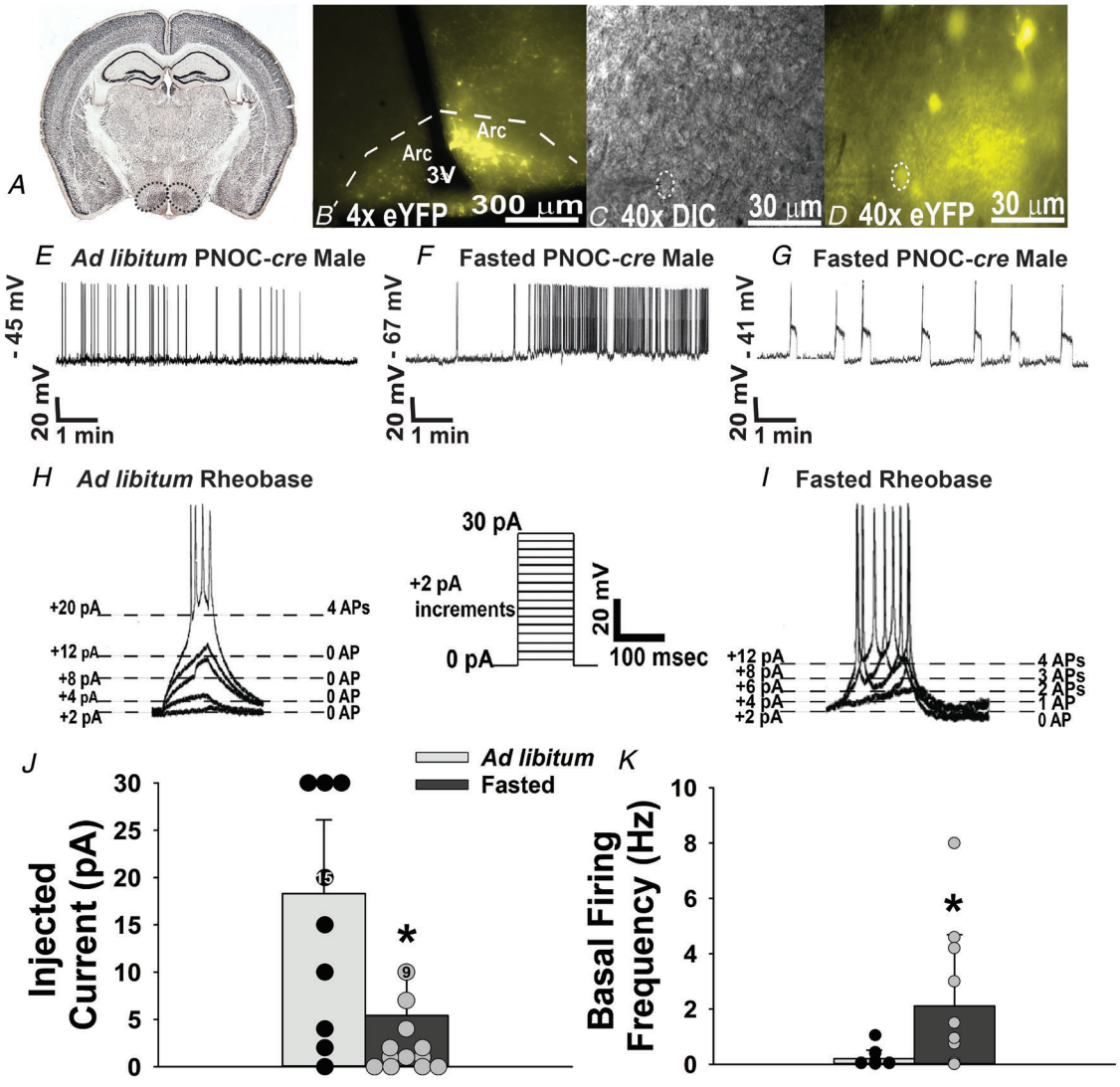

Figure 1. N/OFQ^{ARC} neurones are hyperexcitable under conditions of negative energy balance
A, coronal section illustrating the region of interest. *B*, low power (×4) image of a N/OFQ^{ARC} neurone taken from PNOC-*cre* transgenic mouse. *C* and *D*, differential interference contrast image (×40) of a recorded N/OFQ neurone (*C*) and corresponding eYFP fluorescence from the same neurone (*D*). *E* and *F*, representative current clamp traces from N/OFQ neurones showing baseline firing for *ad libitum*-fed animals and increased firing frequency seen in fasted animals. *G*, representative current clamp trace from an N/OFQ neurone depicting the phasic firing pattern seen in some N/OFQ^{ARC} neurones. *H* and *I*, representative depiction of rheobase thresholds showing the hyperexcitability of N/OFQ^{ARC} neurones under fasted conditions compared to the greater rheobase threshold in cells from the *ad libitum* cohort. *J* and *K*, composite data quantifying the amount of current which necessitates reaching threshold in N/OFQ^{ARC} neurones from both *ad libitum*-fed and fasted animals, as well as the differences in firing frequency of the cells from the *ad libitum*-fed and fasted groups. Bars represent means and lines 1 SD. $^*P < 0.05$; *ad libitum* $n = 23$ cells in 14 slices from 5 animals; fasted $n = 20$ cells in 13 slices from 5 animals; Student's *t* test, relative to *ad libitum* conditions. [Colour figure can be viewed at wileyonlinelibrary.com]

parts (Fig. 1*E* and *F*). In some cases, N/OFQ^{ARC} neurones from both fasted and *ad libitum* cohorts (21% of cells $n = 43$ in total) displayed a phasic firing pattern (Fig. 1*G*). Next, we wanted to quantify the excitability of N/OFQ^{ARC} neurones. Utilizing a protocol whereby the injected current increased in 2-pA increments over 15 steps and the depolarizing response was monitored, we found that the rheobase threshold for *ad libitum*-fed N/OFQ^{ARC} neurones was nearly three-fold that of cells from fasted animals (Fig. 1*H–J*). As such, N/OFQ^{ARC} neurones from *ad libitum*-fed animals exhibited a significantly higher threshold to reach action potential firing compared to fasted animals (Fig. 1*J*; $P = 1.67 \times 10^{-7}$). Additionally, while there was no difference in the resting membrane potential of cells from the *ad libitum*-fed *vs*. the fasted groups (*ad libitum*: -60.7 ± 12.5 mV; fasting: -57.4 ± 14.1 mV; $P = 0.396$), basal firing frequency for N/OFQ^{ARC} neurones from the fasted cohort was significantly greater than basal firing frequency of the *ad libitum*-fed animals (Fig. 1*K*; $P < 0.0001$).

Following the establishment of N/OFQ^{ARC} neuronal hyperactivity being potentiated under conditions of negative energy balance, we sought to further define the electrical behaviour of the observed oscillatory burst firing patterns. Previous research implicates calcium dynamics underlying burst firing mechanisms (Amini et al., 1999; Cain & Snutch, 2013). Therefore, we aimed to test the working hypothesis that these N/OFQ^{ARC} oscillatory burst firing patterns are calcium dependent. N/OFQ^{ARC} neurones were recorded in current clamp with or without the calcium chelator BAPTA added to the electrode's internal solution. Observational recordings monitoring the membrane potential and firing spanned 10 min in length. Of the N/OFQ^{ARC} neurones recorded, there was a significantly greater percentage of burst-firing cells under fasting conditions as compared to *ad libitum*-fed conditions (Fig. 2*A*, *C* and *D*; $P < 0.0001$). In the presence of BAPTA, cells were still capable of firing action potentials, but the oscillatory burst firing pattern was completely abolished (Fig. 2*B* and *E*). Therefore, the phasic firing pattern observed in nearly one-fifth of N/OFQ^{ARC} neurones occurs in a calcium-dependent manner. We also aimed to further characterize differences in the electrical properties of N/OFQ^{ARC} neurones from animals in the sated, *ad libitum*-fed *versus* the fasted state. Negative energy balance increased the frequency of plateau potentials in these oscillatory burst firing incidents compared to the *ad libitum* cohort (Fig. 2*F*; $P = 0.048$). Additionally, the oscillatory burst duration was significantly longer in N/OFQ^{ARC} neurones from the fasted cohort when compared to the *ad libitum* cohort (Fig. 2*G*; $P = 0.040$). By contrast, there was no significant differences in either the plateau potential firing frequency (Fig. 2*H*; $P = 0.734$) or the magnitude of these plateau potentials (Fig. 2*I*; $P = 0.614$). Taking these data into account, it can be concluded that the oscillatory firing pattern of N/OFQ^{ARC} neurones is calcium dependent, and negative energy balance promotes the hyperexcitability of N/OFQ^{ARC} neurones by potentiating the duration of these bursting incidences while increasing the frequency of these plateau potentials.

Stimulation of N/OFQ^{ARC} neurones inhibits POMC^{ARC} neurones, which is potentiated under conditions of negative energy balance

Now that we have characterized the electrical behaviour of N/OFQ^{ARC} neurones, we wanted to determine whether stimulation of these N/OFQ^{ARC} neurones would elicit greater inhibitory effects in downstream neuronal targets under conditions of negative energy balance. On the other end of the energy balance continuum, previous research demonstrated that inhibitory actions of N/OFQ$^{ARC/VTA}$ neurones are maladaptively enhanced under DIO conditions (Hernandez et al., 2019, 2021). Therefore, we developed the working hypothesis that inhibitory input from N/OFQ^{ARC} onto POMC^{ARC} neurones would be adaptively potentiated under negative energy balance.

To further affirm whether negative energy balance facilitates the hyperexcitability of N/OFQ^{ARC} neurones, we employed chemogenetic techniques to stimulate or inhibit N/OFQ^{ARC} neurones. We initially set out to conduct *in vitro* chemogenetic studies in hypothalamic slices from animals injected with one of hM3D(Gq) DREADD coupled to mCherry, an mCherry blank control, or hM4D(Gi) mCherry-coupled DREADD AAVs, and record from mCherry-fluorescing N/OFQ^{ARC} neurones (Fig. 3*A–C*). As can be seen in the representative trace in Fig. 3*D*, bilateral injection of hM3D(Gq) DREADD coupled to mCherry, an excitatory DREADD, produced a reversible depolarization and increase in burst firing in recorded N/OFQ^{ARC} neurones upon bath application of CNO (5 μM). This effect that was not emulated in the control mCherry-injected cohort, which displayed little to no change in membrane potential and firing (Fig. 3*E*). In contrast, N/OFQ^{ARC} neurones recorded from hM4D(Gi) DREADD-injected animals expressed frequent firing until the application of CNO, which caused a cessation in firing and reversible hyperpolarization (Fig. 3*F*). Composite data show the chemostimulation and chemoinhibition of N/OFQ^{ARC} neurones elicited significantly greater depolarizing and hyperpolarizing changes in membrane potential, respectively, relative to the change in membrane potential in cells from the mCherry control-injected animals (Fig. 3*G*; $P = 0.001$). It can be discerned from these data that, indeed, we can chemogenetically excite and inhibit N/OFQ^{ARC} neurones in a reliable and reproducible manner. Fasting conditions modulates the excitability of N/OFQ^{ARC} neurones, and

this hyperexcitability of N/OFQ^{ARC} neurones is abolished upon inhibition.

We then wanted to see whether this fasting-induced hyperexcitability of N/OFQ^{ARC} neurones functionally translated into enhanced inhibitory tone onto downstream POMC^{ARC} neurones. Thus, double transgenic PNOC-*cre*/eGFP POMC mice were injected into the ARC with an excitatory DREADD coupled to mCherry or an mCherry blank control. We recorded from eGFP-fluorescing POMC^{ARC} neurones in voltage clamp and chemogenetically stimulated mCherry-expressing N/OFQ^{ARC} neurones (Fig. 4*A*–*E*) with CNO (5 μM). Recordings were taken from hypothalamic slices from either *ad libitum*-fed or fasting treatment groups. Chemogenetic stimulation of N/OFQ^{ARC} neurones in the *ad libitum* cohort induced a reversible outward current

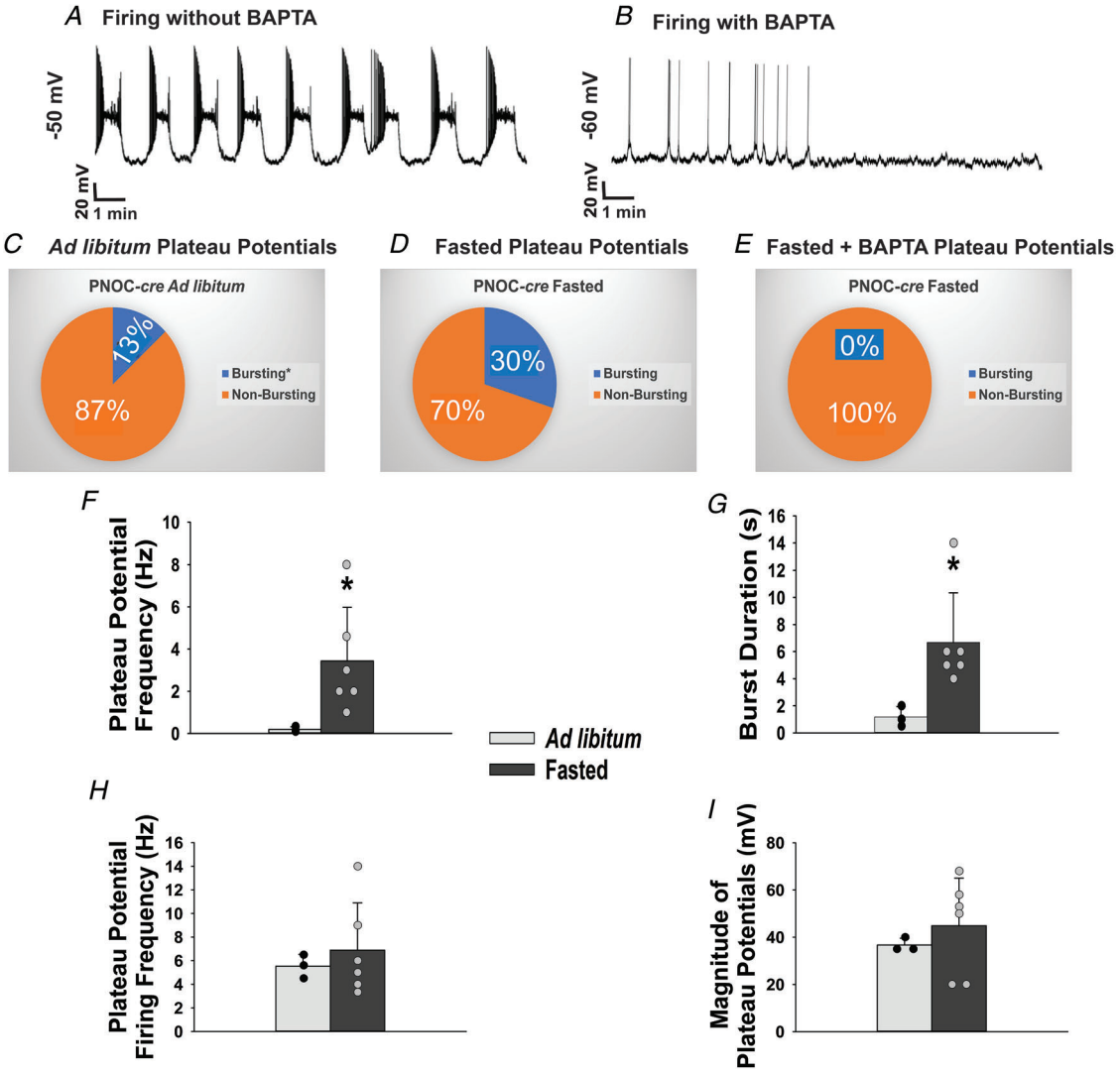

Figure 2. Phasic firing occurring in N/OFQ^{ARC} neurones is calcium dependent and potentiated by negative energy balance
A and *B*, representative current clamp traces of N/OFQ neurones exhibiting oscillatory firing patterns (*A*), and the mitigation of incidences of burst firing with the addition of calcium chelator BAPTA (*B*). *C*–*E*, pie charts displaying the proportion of N/OFQ^{ARC} neurones that exhibit oscillatory firing patterns. *C*, 3 of 23 neurones recorded from *ad libitum* conditions exhibited oscillatory firing patterns. *D* and *E*, no significant difference in incidences of phasic firing and conventional firing under fasted conditions (*D*, 6 of 20 neurones recorded) *versus* in the presence of BAPTA (*E*, 0 of 9 neurones displayed oscillatory firing pattern). *Sample falls beyond decision limits. *F* and *G*, composite data highlighting the potentiation of the plateau potential frequency (*F*), and the duration of bursting (*G*) under conditions of negative energy balance. *H* and *I*, composite data depicting the similarity of the firing frequency and magnitude of plateau potentials between *ad libitum*-fed and fasted groups. Bars represent means and lines 1 SD. *$P < 0.05$; *ad libitum* $n = 3$ cells in 3 three slices from 2 animals; fasted $n = 6$ cells in 6 slices from 5 animals; Student's *t* test, relative to *ad libitum* conditions. [Colour figure can be viewed at wileyonlinelibrary.com]

in POMC^{ARC} neurones (Fig. 4*F*), whereas those in the fasted cohort exhibited a more robust outward current, indicative of greater inhibition of these POMC^{ARC} neurones (Fig. 4*H*). By contrast, CNO was without effect in slices from the mCherry blank control group, indicating that the outward currents produced were dependent on chemogenetic stimulation of N/OFQ^{ARC} neurones (Fig. 4*G*). The chemogenetically induced outward currents caused by the endogenous release of N/OFQ reversed membrane polarity in both *ad libitum* and fasted groups at approximately −90 mV, which is the Nernst equilibrium constant for potassium conductance (Fig. 4*I* and *J*). As can be seen from the composite data, the fasted group exhibited a greater change in membrane current (measured by subtracting the baseline holding current from the new steady-state current observed in the presence of CNO) and slope conductance (measured via linear regression between −60 and −80 mV) following application of CNO compared to the *ad libitum* group (Fig. 4*K*, $P < 0.0001$; and Fig. 4*L*, $P < 0.0001$). These results indicate chemostimulation of N/OFQ^{ARC} neurones inhibits POMC^{ARC} neurones in a manner that is amplified under conditions of negative energy balance.

We also utilized optogenetic stimulation of N/OFQ^{ARC} neurones to further test whether fasting induces a more pronounced inhibitory N/OFQ tone onto POMC^{ARC} neurones. Double transgenic PNOC-*cre*/eGFP POMC mice received ARC injections of AAV constructs containing eYFP-tagged ChR2. eYFP/ChR2-expressing N/OFQ^{ARC} neurones (Fig. 5*B* and *E*) were optogenetically stimulated and the postsynaptic response was recorded in eGFP-fluorescing POMC^{ARC} neurones (Fig. 5*A*, *C*

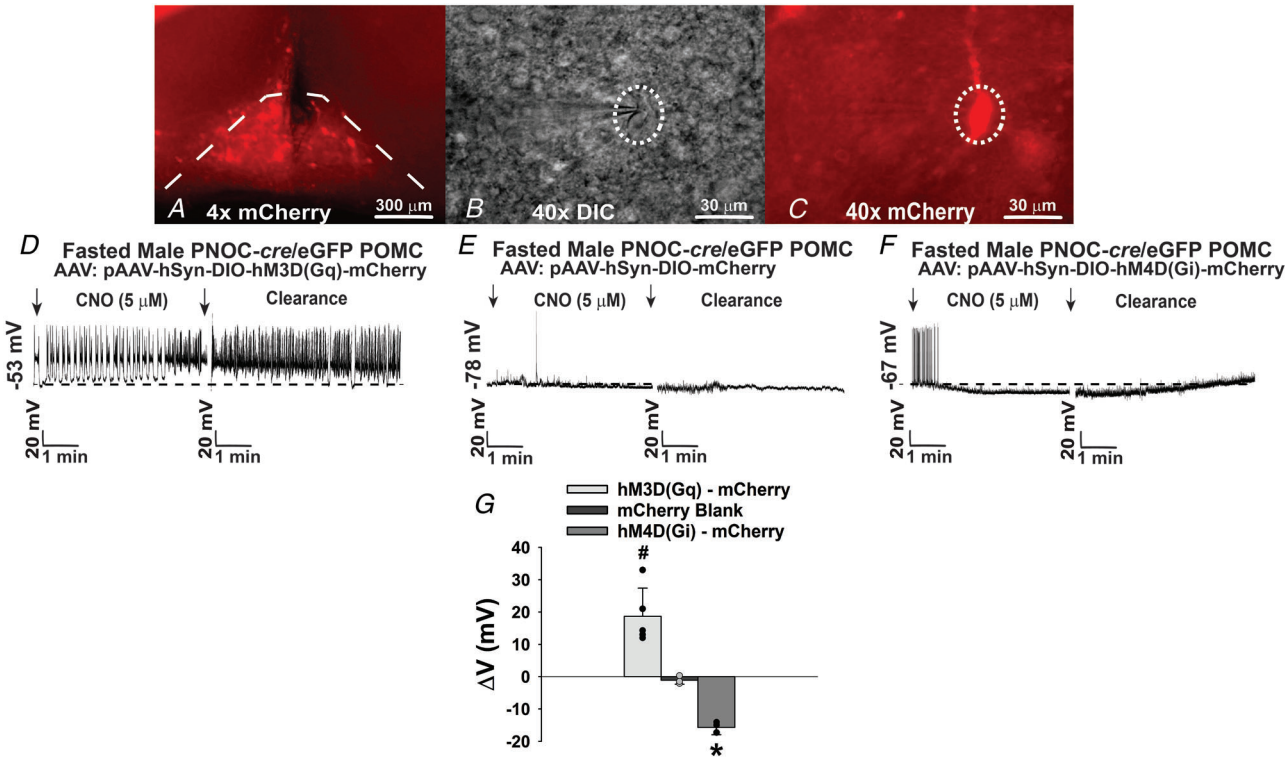

Figure 3. Validation of the *in vitro* chemogenetic approach seen in N/OFQ^{ARC} neurones from DREADD-injected male PNOC-*cre* animals
A–C, representative photomicrograph of mCherry fluorescing N/OFQ^{ARC} neurones in low power (×4) (*A*), a high power image (×40) DIC image of a recorded N/OFQ neurone (*B*), and a high power (×40) image depicting its corresponding mCherry fluorescence (*C*). *D–F*, representative current clamp traces of N/OFQ^{ARC} neurones obtained from transgenic PNOC-*cre* mice injected bilaterally with mCherry-tagged, Gq-coupled excitatory DREADD (*D*), mCherry control (*E*), and mCherry- tagged Gi-coupled inhibitory DREADD (*F*). Current clamp traces depict the depolarization and hyperexcitability of firing associated with stimulation of N/OFQ^{ARC} neurones, no change in membrane potential or firing without the association of DREADDs, and the hyperpolarization and cessation of firing associated with inhibition of N/OFQ^{ARC} neurones. *G*, composite data depicting the significantly depolarizing change in membrane potential upon chemostimulation of N/OFQ^{ARC} neurones, as well as the hyperpolarization seen upon chemoinhibition of these cells. Bars represent means, and lines 1 SD of the induced change upon application of CNO (*D*); one-way ANOVA, #$P < 0.05$, relative to Hm4D(Gi), *$P < 0.05$ relative to mCherry blank control. Control $n = 3$ cells in 2 slices from 1 animal; excitatory DREADD $n = 5$ cells in 3 slices from 1 animal; inhibitory DREADD $n = 3$ cells in 2 slices from 1 animal. [Colour figure can be viewed at wileyonlinelibrary.com]

and *D*). Recordings were conducted in voltage clamp in both *ad libitum* and fasted groups. We have shown previously that optogenetic stimulation of N/OFQ^{ARC} neurones produces a frequency-dependent increase in cell firing, and the endogenous N/OFQ released inhibits POMC^{ARC} neurones, effects which are not seen in animals injected with the eYFP blank control (Hernandez et al., 2021). Thus, currently we observed that photostimulation of N/OFQ^{ARC} neurones elicited a modest, reversible outward current in POMC^{ARC} neuro-

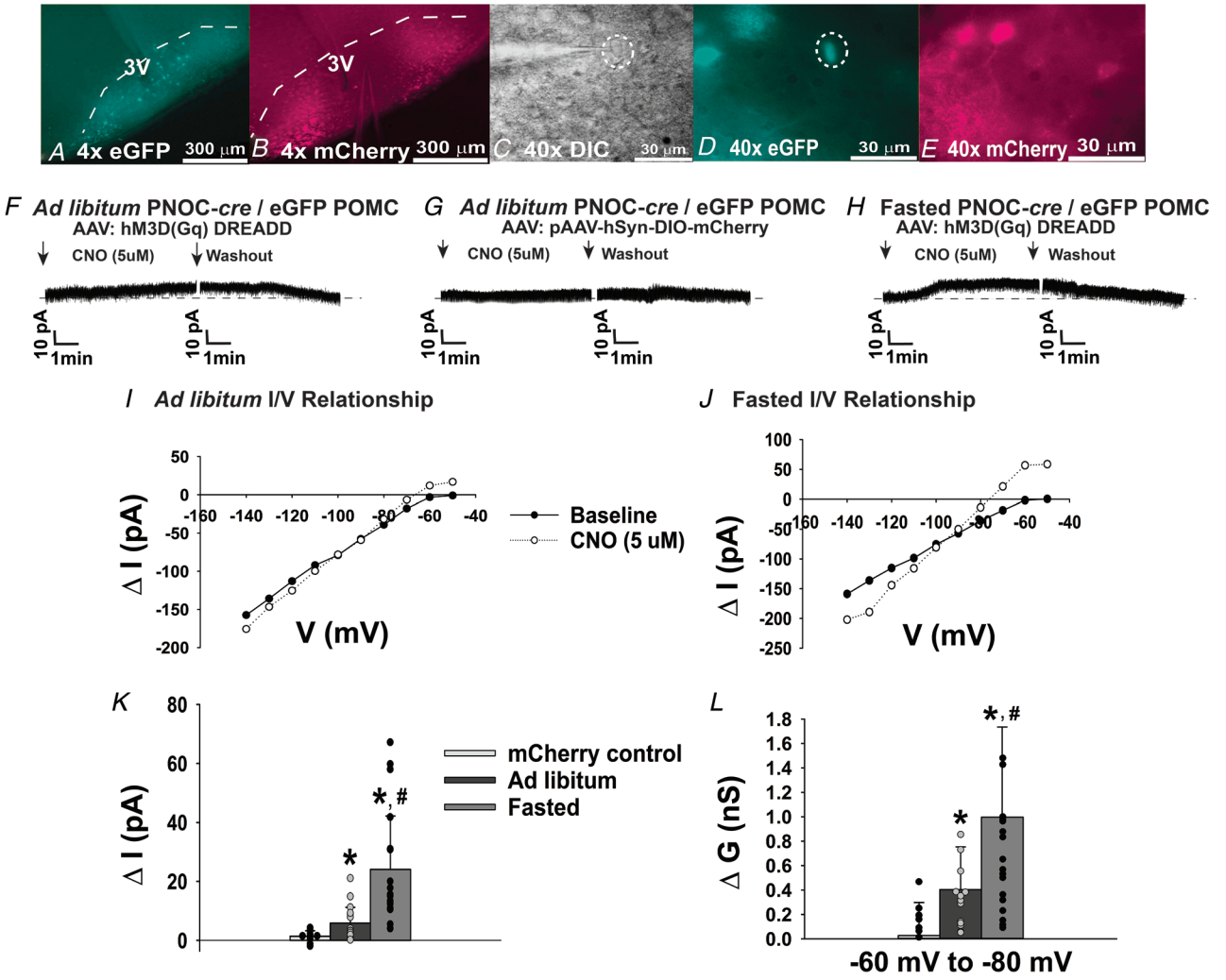

Figure 4. Chemogenetic stimulation of N/OFQ^{ARC} neurones produces an outward current in male POMC^{ARC} neurones, actions which are amplified under negative energy balance
A–E, representative photomicrograph. *A*, low power (×4) image of eGFP-fluorescing POMC^{ARC} neurones taken from double transgenic PNOC-*cre*/eGFP-POMC mice. *B*, low power (×4) image depicting either Gq mCherry tagged excitatory DREADD- or mCherry blank control-expressing N/OFQ^{ARC} neurones. *C* and *D*, differential interference contrast image (×40) of a recorded POMC neurone (*C*) and corresponding eGFP fluorescence from the same neurone (*D*). *E*, mCherry-expressing N/OFQ^{ARC} neurones within the vicinity of the recorded POMC^{ARC} neurone. *F–H*, representative voltage clamp traces depicting the modest outward current in the *ad libitum* group elicited in POMC^{ARC} neurones via activation of N/OFQ^{ARC} neurones, and the robust outward current in the fasting group receiving the same treatment. Additionally, the mCherry blank control group displays no change in current, assuring that the outward currents are only elicited in cells from the DREADD-injected animals, and therefore a consequence of stimulation of N/OFQ^{ARC} neurones. *I* and *J*, current–voltage relationships between baseline and application of CNO, displaying the reversal potential for potassium in both groups and a greater change in slope conductance for the fasting group. *K* and *L*, composite data depicting the significantly greater change in current and slope conductance (measured between −60 and −80 mV) for POMC^{ARC} neurones under conditions of negative energy balance as compared to the *ad libitum* group and mCherry blank control. Bars represent means and lines 1 SD. $^{*}P < 0.05$ relative to control, $\#P < 0.05$, one-way ANOVA/LSD, relative to *ad libitum*. Control $n = 13$ cells in 7 slices from 2 animals; *ad libitum* $n = 26$ cells in 16 slices from 5 animals; fasted $n = 24$ cells in 14 slices from 5 animals. [Colour figure can be viewed at wileyonlinelibrary.com]

nes taken from the *ad libitum* group (Fig. 5*F*), and a more robust outward current in the fasted conditions was observable (Fig. 5*G*). In both *ad libitum*-fed and fasted groups, optogenetically induced outward currents caused by the endogenous release of N/OFQ reversed POMC membrane polarity at approximately −90 mV. However, as with the chemogenetic experiment, the fasted group displayed POMC^{ARC} neurones that had a larger change in slope conductance compared to their *ad libitum* counterparts (Fig. 5*H* and *I*). Additionally, negative energy balance facilitated a significantly greater change in both current and conductance than in the *ad libitum*-fed condition (Fig. 5*J*, $P = 0.019$; and Fig. 5K, $P = 0.006$). Together, these findings corroborate those which were seen in the chemogenetic studies, indicating that postsynaptic actions of N/OFQ^{ARC} neurones inhibit

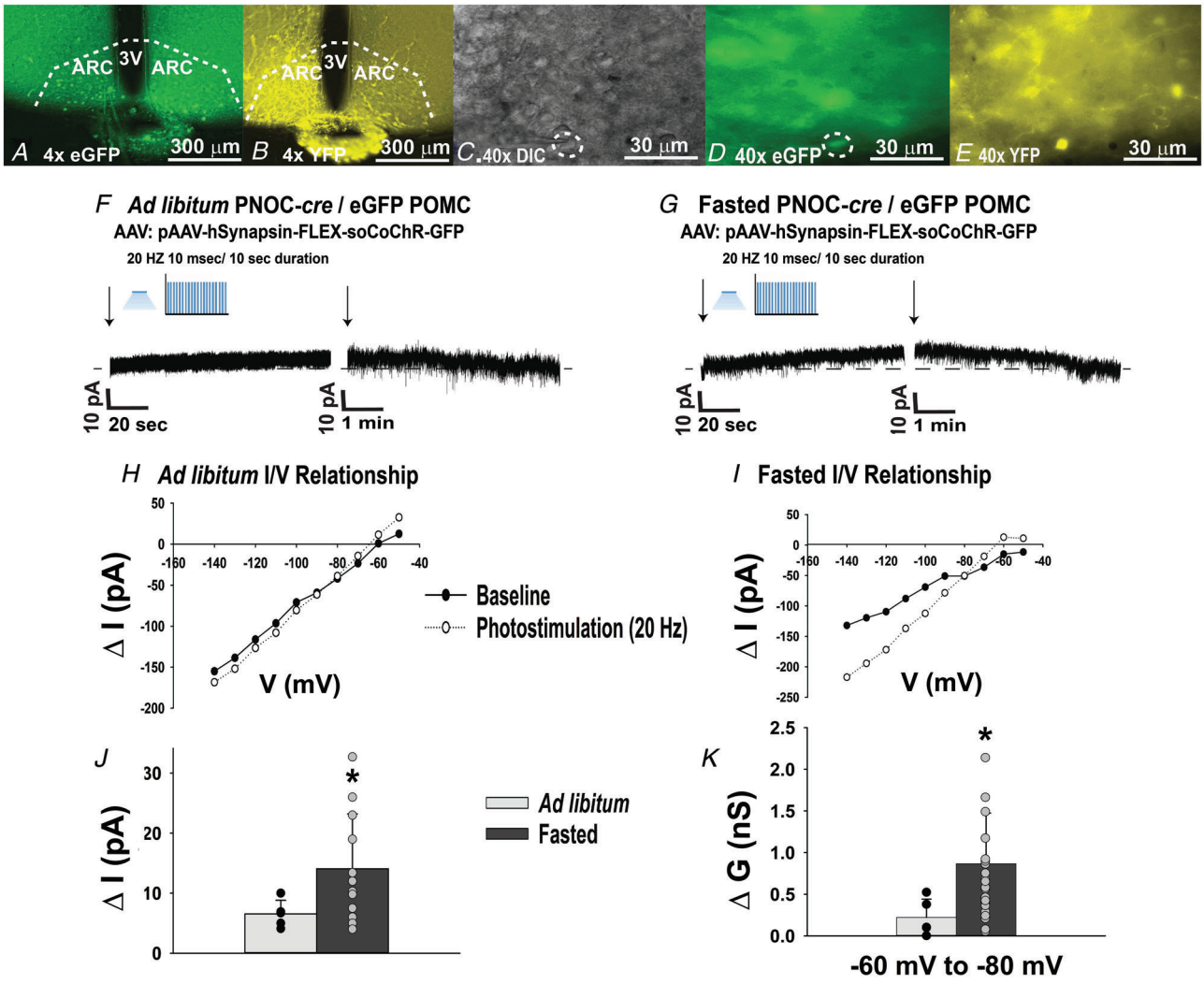

Figure 5. Optogenetic stimulation of N/OFQ^{ARC} neurones produces a reversible outward current in male POMC^{ARC} neurones, with a heightened response under negative energy balance
A–D, representative photomicrographs. *A*, low power (×4) image of eGFP-fluorescing POMC^{ARC} neurones. *B*, low power (×4) image of ChR2/eYFP-tagged N/OFQ^{ARC} neurones. *C* and *D*, high power (×40) DIC image depicting a recorded POMC neurone (*C*) and eGFP fluorescence of the same neurone (*D*). *E*, eYFP-fluorescing N/OFQ^{ARC} cell bodies and fibres in the vicinity of the recorded POMC^{ARC} neurone. *F* and *G*, representative voltage clamp traces depicting inhibitory outward currents of POMC^{ARC} neurones elicited by optogenetic stimulation under *ad libitum*-fed (*F*) and fasted (*G*) conditions. *H* and *I*, current–voltage relationships between baseline and photostimulation of N/OFQ^{ARC} neurones depicting a reversal potential aligning with potassium conductance and a greater change in slope conductance under negative energy balance. *J* and *K*, the composite data in the two graphs summarizing the inhibitory effects of endogenously released N/OFQ invokes on current and conductance (measured between −60 and −80 mV), which are greater under conditions of negative energy balance. Bars represent means and lines 1 SD. $^*P < 0.05$ relative to *ad libitum* conditions; *ad libitum* $n = 7$ cells in 7 slices from 4 animals; fasted $n = 13$ cells in 13 slices from 5 animals; Student's *t* test. [Colour figure can be viewed at wileyonlinelibrary.com]

POMC^{ARC} neurones to a greater degree under conditions of negative energy balance.

The fasting-induced potentiation of the inhibitory effects of N/OFQ^{ARC} neurones on POMC^{ARC} neurones is sexually differentiated and attenuated by E_2 in females

Oestrogen uncouples $G_{i/o}$ receptors from activating GIRK channels (Kelly & Wagner, 1999), and notably, previous research depicts that this steroid hormone attenuates the N/OFQ-induced GIRK channel activation in POMC neurones (Borgquist et al., 2013). Therefore, we tested the working hypothesis that the magnitude of inhibitory actions of N/OFQ^{ARC} neurones will be sex dependent. PNOC-*cre*/eGFP mice were injected with excitatory DREADD and separated into groups based on sex. All females were ovariectomized (OVX females). During electrophysiological voltage clamp recordings, N/OFQ^{ARC} neurones were chemogenetically stimulated with bath application of CNO (5 μM), and hypothalamic slices from OVX females were treated with either E_2 (100 nM) or a punctilious ethanol (EtOH) vehicle (0.01% v/v). Chemogenetic stimulation of N/OFQ^{ARC} neurones produced a reversible outward current in recorded POMC^{ARC} neurones (Fig. 6*A*–*C*). However, the magnitude of inhibition varied based on sex. POMC^{ARC} neurones recorded from males and especially those from EtOH-treated slices from OVX females exhibited an observably larger outward current (Fig. 6*A* and *B*) than POMC^{ARC} neurones from OVX females recorded in E_2-treated hypothalamic slices (Fig. 6*C*), which exhibited a very modest outward current. Quantification of the change in current illustrated that the chemogenetically induced inhibition of POMC^{ARC} neurones in E_2-treated slices from OVX females was significantly less than that seen in EtOH-treated slices from OVX females or in males (Fig. 6*D*, $P = 0.018$; and Fig. 6*E*, $P = 0.012$). These findings indicate that the presence of E_2 in females attenuates the inhibitory actions of endogenously released N/OFQ; rendering those lacking E_2 more susceptible to these inhibitory effects elicited by N/OFQ.

The fasting-induced hyperexcitability of N/OFQ^{ARC} neurones elicits a greater endogenous tonic inhibitory tone onto POMC^{ARC} neurones

Our first experiment depicted that N/OFQ^{ARC} neurones were hyperexcitable under conditions of negative energy balance. These results led us to our next working hypothesis, that N/OFQ^{ARC} neurones invoke an endogenous inhibitory tone onto POMC^{ARC} neurones under

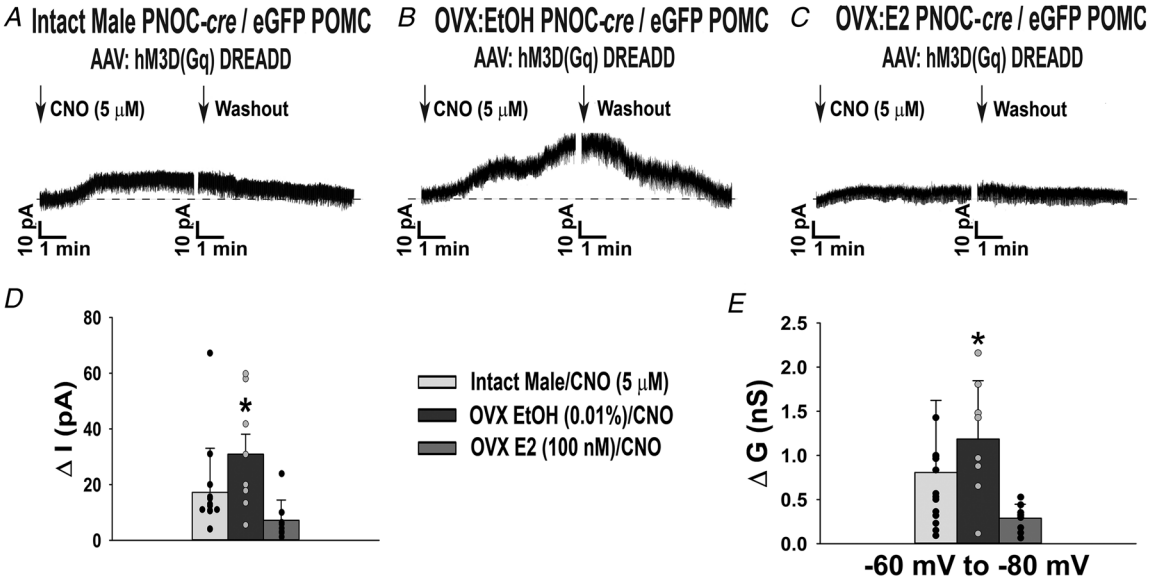

Figure 6. Chemogenetic stimulation of N/OFQ^{ARC} neurones under fasting conditions elicits a robust and reversible outward current that is sex and E_2 dependent
A-*C*, representative voltage clamp traces depicting the robust outward currents during recordings of POMC^{ARC} neurones in hypothalamic slices collected from males (*A*), and slices from OVX females treated for ∼5 min with EtOH vehicle (*B*), as well as a very modest outward current in slices treated with E_2 for ∼5 min (*C*). *D* and *E*, composite data illustrating E_2 markedly attenuated the inhibitory effects as depicted by a modest change in current and conductance (measured between −60 and −80 mV) compared to males and EtOH vehicle-treated slices from OVX females. Bars represent means and lines 1 SD. *$P < 0.05$ relative to E_2 treatment; E_2 n = 9 cells in 5 slices from 2 animals; intact male n = 14 cells in 9 slices from 3 animals; EtOH n = 8 cells in 5 slices from 2 animals; Student's t test.

these conditions. To test this hypothesis, we utilized both pharmacological and chemogenetic means. For the pharmacological protocol, eGFP-POMC mice were utilized and randomly assigned to either *ad libitum*-fed or fasted groups. Voltage clamp recordings were conducted on eGFP- fluorescing POMC^{ARC} neurones in hypothalamic slices (Fig. 7*A*–*C*). Bath application of NOP receptor peptide antagonist UFP-101 (100 nM) caused a reversible inward current in the POMC^{ARC} neurones from the *ad libitum* cohort (Fig. 7*D*), which was

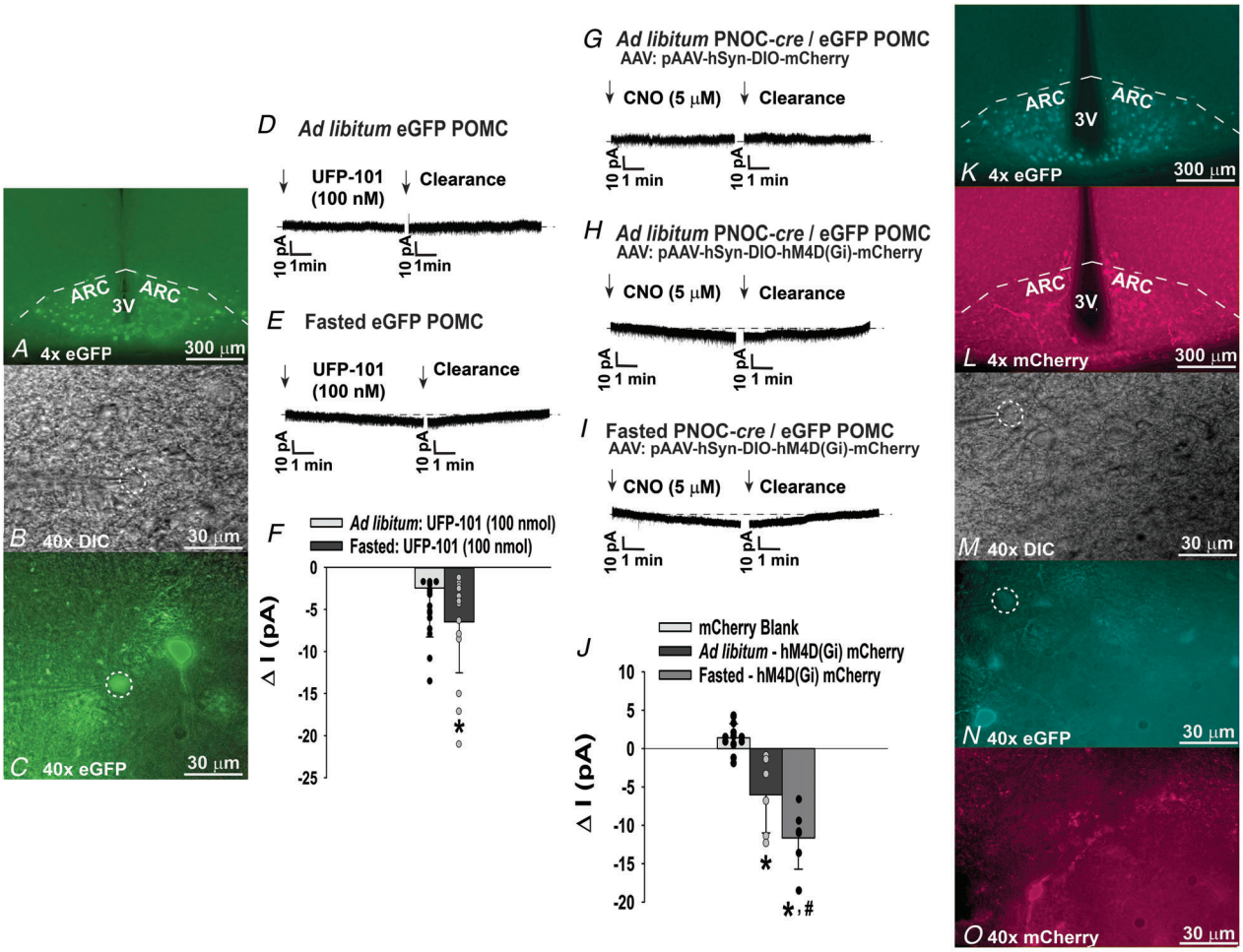

Figure 7. Inhibition of the N/OFQ–NOP receptor system induces a reversible inward current that is potentiated under negative energy balance
A–*C*, representative photomicrographs. *A*, low power (×4) image of eGFP-fluorescing POMC^{ARC} neurones. *B* and *C*, high power (×40) DIC image of a recorded POMC^{ARC} neurone (*B*) and the eGFP fluorescence of the same neurone (*C*). *D* and *E*, representative voltage clamp traces depicting the inward currents elicited by antagonism of the NOP receptor under sated, *ad libitum*-fed conditions (*D*), and the potentiation under negative energy balance (*E*). *F*, composite data depicting negative energy balance elicits a significantly greater change in current compared to *ad libitum* conditions. $^*P < 0.05$ relative to *ad libitum*; *ad libitum* $n = 23$ cells in 13 slices from 5 animals; fasted $n = 18$ cells in 12 slices from 5 animals; Student's *t* test. *G*–*I*, representative traces depicting chemogenetic inhibition of N/OFQ^{ARC} neurones inducing a reversible inward current in *ad libitum* (*H*) conditions, which is potentiated under fasted conditions (*I*); inhibition of this system is dependent on presence of DREADD in N/OFQ^{ARC} neurones, as there is no CNO-induced change in current in the mCherry blank control group (*G*). *J*, composite data depicting inward currents are significantly greater in the fasted group. $^*P < 0.05$ relative to control, $\#P < 0.05$ relative to control; control $n = 13$ cells in 7 slices from 2 animals; *ad libitum* $n = 6$ cells in 3 slices from 1 animal; fasted $n = 6$ cells in 3 slices from 1 animal; one-way ANOVA/LSD. Bars represent means and lines 1 SD of the change in membrane current obtained from a mixture of male and OVX female animals balanced across the different treatment and energy balance conditions. *K*–*O*, representative photomicrographs. *K* and *L*, low power (×4) image of eGFP-fluorescing POMC^{ARC} neurones and N/OFQ^{ARC} mCherry fluorescing neurones (*K*) and fibres (*L*). *M* and *N*, high power (×40) DIC image of a recorded POMC^{ARC} neurone (*M*) and eGFP fluorescence of the same neurone (*N*). *O*, high power (×40) image of mCherry-fluorescing N/OFQ^{ARC} cell bodies and fibres within the same vicinity of the recorded POMC^{ARC} neurone. [Colour figure can be viewed at wileyonlinelibrary.com]

potentiated in those from the fasted cohort (Fig. 7*E*). Quantification of current deviance from baseline following bath application of UFP-101 depicted a significantly greater change in current under conditions of negative energy balance compared to homeostatic *ad libitum* conditions (Fig. 7*F*; $P = 0.044$). With the few PNOC-*cre*/eGFP POMC mice left available, we attempted further verification of our pharmacological findings. Subjects were injected into the ARC with either inhibitory DREADD or an mCherry-tagged blank control. Inhibitory DREADD-injected animals were further randomly assigned to either *ad libitum*-fed or fasted groups. N/OFQ^{ARC} mCherry-expressing neurones (Fig. 7*L* and *O*) were chemogenetically inhibited with CNO (5 μM) and the resultant postsynaptic effects were recorded in eGFP-fluorescing POMC^{ARC} neurones (Fig. 7*K*, *M* and *N*). POMC^{ARC} neurones displayed inward currents in the *ad libitum* group upon chemogenetic inhibition of N/OFQ^{ARC} neurones (Fig. 7*H*), an effect that was potentiated under fasting conditions (Fig. 7*I*). The mCherry-tagged control group displayed little to no change in current following bath application of CNO (Fig. 7*G*), indicating the inward currents in POMC^{ARC} neurones were a result of chemogenetic inhibition of N/OFQ^{ARC} neurones rather than actions solely from CNO. Quantification of current deviance from baseline upon application of CNO depicted POMC^{ARC} neurones in the fasted group experiencing the greatest change in current, followed by the *ad libitum* group (Fig. 7*J*; $P < 0.0001$). These results corroborate the findings that negative energy balance potentiates the inhibitory effects of N/OFQ, and when the N/OFQ–NOP receptor system signalling is abrogated, the degree of disinhibition of POMC^{ARC} neurones is larger as compared to the *ad libitum* group. This reveals that negative energy balance accentuates the endogenous tonic inhibitory N/OFQ tone onto POMC^{ARC} neurones.

In vivo intra-ARC administration of N/OFQ and chemogenetic excitation of N/OFQ^{ARC} neurones both elicit voracious hyperphagia upon re-feeding under conditions of negative energy balance, whereas chemogenetic inhibition does the opposite

Administration of N/OFQ *in vivo* is implicated in increased adiposity and hyperphagia (Hernandez et al., 2019; Olszewski & Levine, 2004). Based on our data depicting the hyperexcitability of N/OFQ^{ARC} neurones under conditions of negative energy balance, we aimed to test our hypothesis that intra-ARC administration of N/OFQ peptide under conditions of negative energy balance would promote a more vigorous rebound hyperphagia during the re-feed period following fasting.

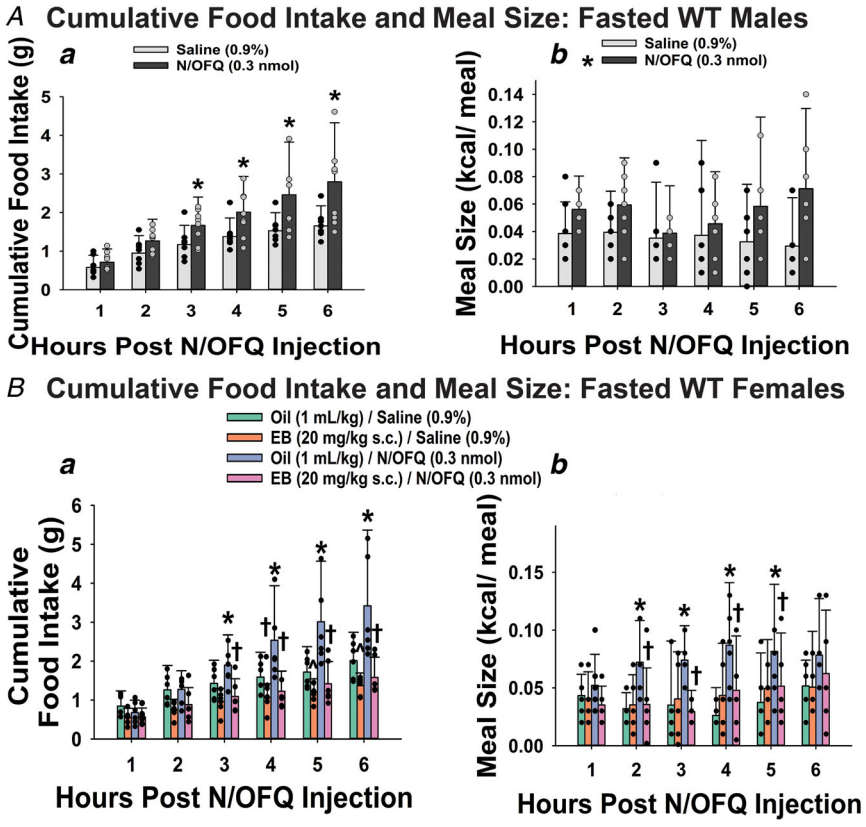

Figure 8. Intra-ARC administration of N/OFQ induces an increase in rebound hyperphagia and meal size upon re-feeding under conditions of negative energy balance
Aa, composite data depicting that treatment with N/OFQ promoted a significantly more robust hyperphagic response across the 6 h re-feed period. $^*P < 0.05$ relative to saline. *Ab*, composite data illustrating exogenous N/OFQ promoted increased meal size. $^*P < 0.05$ relative to saline-treated group; saline $n = 7$ animals, N/OFQ $n = 8$ animals. *Ba*, composite data depicting N/OFQ elicits an elevated hyperphagic response in OVX oil vehicle-treated females, and this N/OFQ-induced hyperphagia is attenuated in the presence of E_2. $^*P < 0.05$ relative to saline; †$P < 0.05$ relative to oil. *Bb*, composite data depicting exogenous N/OFQ promotes an increase in meal size in OVX oil vehicle-treated females, and this increase in meal size is diminished by E_2. $^*P < 0.05$ relative to saline; †$P < 0.05$ relative to oil; WT oil/saline vehicle $n = 6$ animals; WT EB/saline $n = 6$ animals; WT EB/N/OFQ $n = 6$ animals; WT oil/N/OFQ $n = 6$ animals. [Colour figure can be viewed at wileyonlinelibrary.com]

Wild type male mice were surgically outfitted with guide cannulas positioned just above the ARC to allow for intra-ARC administration of the N/OFQ peptide (0.3 nmol) or its saline vehicle (0.9%) at the beginning of the re-feed period. Intra-ARC administration of N/OFQ promoted an increase in cumulative food intake over the 6 h re-feed period in comparison to their saline vehicle-treated counterparts (Fig. 8*Aa*; $P < 0.0001$). Additionally, N/OFQ administration promoted increased meal size compared to the saline-treated group (Fig. 8*Ab*; $P < 0.0001$). OVX females treated with intra-ARC injections of N/OFQ (0.3 nmol) and subcutaneous (s.c.) injections of sesame oil displayed a similar trend in cumulative food intake and meal size observed in their male counterparts. This incrementally increasing cumulative food intake across the 6 h re-feed period, and overall increase in meal size induced by exogenous N/OFQ, was attenuated by EB (20 μg/kg, s.c.) (Fig. 8*Ba*, $P < 0.0001$; and Fig. 8*Bb*, $P < 0.0001$). Taking these data into consideration, it is evident that N/OFQ promotes a more sustained hyperphagic response during the 6 h re-feed period, coupled with a robust increase in meal size. These effects are sex and hormone dependent as the present of E_2 markedly attenuates the N/OFQ-induced hyperphagia as seen in the oil vehicle-treated OVX females. Lastly, we employed chemogenetic means to excite and inhibit N/OFQ neurones via AAV injection of hM3D(Gq)-mCherry excitatory DREADD and C21 (0.3 nmol, s.c.) to assay the behavioural effects endogenous N/OFQ elicits during the re-feed period following a fast. Following s.c. injection of C21 (used in lieu of CNO as the latter is a prodrug *in vivo* that is converted to the antipsychotic drug clozapine, which then activates DREADDs; Gomez et al., 2017) at 08.00 h, fasted PNOC-*cre* animals exhibited an increased cumulative food intake (Fig. 9*Aa*; $P < 0.0001$) and an overall significant increase in meal size (Fig. 9*Ab*; $P < 0.0001$) compared to the WT counterparts. This was associated with a robust elevation in c-fos expression in the ARC (Fig. 9*B–F*; $P = 0.003$). Moreover, *in vivo* chemoinhibition of N/OFQ^{ARC} neurones attenuated the rebound hyperphagia seen upon re-feeding (Fig. 10*A*; $P < 0.0001$). This was associated with a modest yet statistically insignificant reduction in meal size (Fig. 10*B*; $P = 0.067$). Collectively, these data correspond with the *in vivo* exogenous administration of N/OFQ (0.3 nmol), and solidify that under fasted conditions, N/OFQ induces a pronounced and sustained rebound hyperphagia and increase in meal size during the re-feed period following the fast.

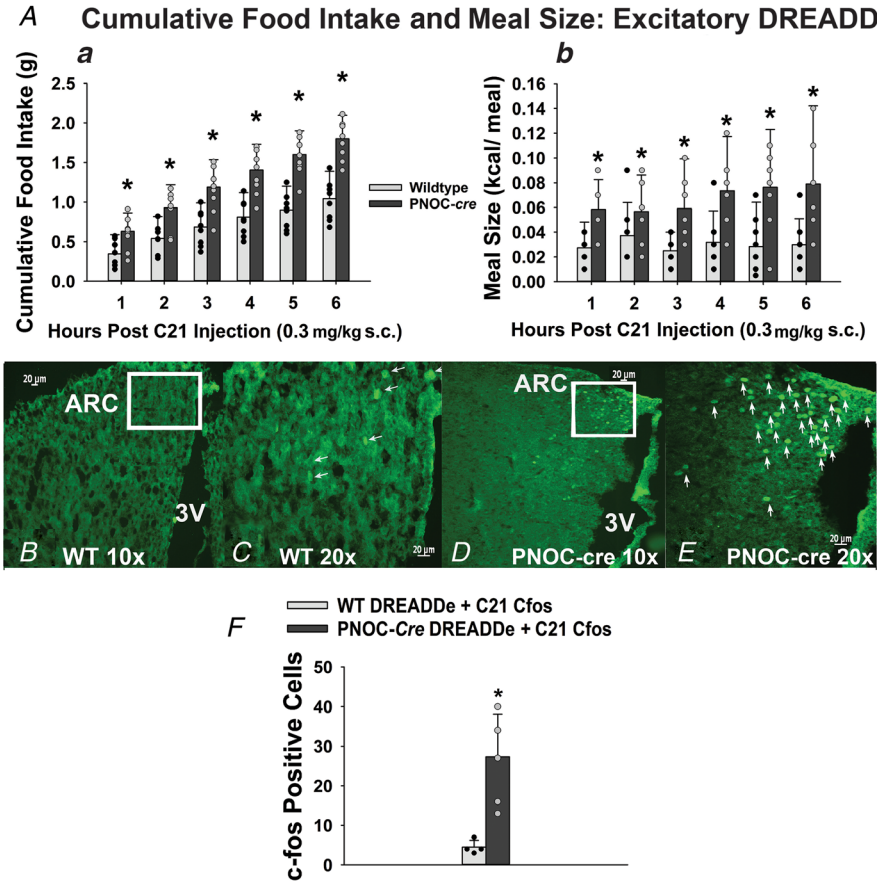

Figure 9. Cre-dependent chemoexcitation of N/OFQ neurones via subcutaneous administration of C21 promotes sustained rebound hyperphagia and increased meal size and c-fos expression under fasted conditions
Aa, composite data depicting C21 promotes a significant increase in cumulative food intake across the 6 h re-feed period. $^*P < 0.05$, relative to wild-type (WT). *Ab*, composite data illustrating chemoexcitation of N/OFQ neurones promotes an overall significant increase in meal size. $^*P < 0.05$, relative to WT; WT $n = 8$ animals; PNOC-*cre* $n = 8$ animals. *B–F*, photomicrographs illustrating c-fos expression at ×10 (*B* and *D*) and ×20 (*C* and *E*) in slices from WT and PNOC-*cre* animals 2 h following C21 treatment, while the bar graph in *F* shows the robust increase in c-fos expression caused by C21 seen in the transgenic subjects. $^*P < 0.05$, relative to WT; WT $n = 5$ animals; PNOC-*cre* $n = 5$ animals. [Colour figure can be viewed at wileyonlinelibrary.com]

Discussion

This study demonstrates the impact that a disruption in energy balance has on the feeding circuitry in the hypothalamus. Under fasting conditions, electrical behaviour of N/OFQ^{ARC} neurones displays heightened sensitivity, and this heightened sensitivity promotes greater inhibition of POMC^{ARC} neurones. This increased inhibition of POMC^{ARC} neurones promotes appetitive behaviour, and this behaviour is exemplified by a more robust hyperphagic effect during the feeding period following a fast. Additionally, the extent of inhibition is dependent on the presence of sex hormones, as evidenced by the fact that E_2 markedly attenuates the inhibitory actions of N/OFQ on POMC^{ARC} neurones.

Negative energy balance promotes hyperexcitability of N/OFQ^{ARC} neurones in a calcium-dependent manner

We have demonstrated that excitability of N/OFQ^{ARC} neurones is increased under negative energy balance. Observational recordings of N/OFQ^{ARC} neurones depicted increased firing frequency in N/OFQ^{ARC} neurones examined from fasted animals compared to *ad libitum*-fed animals. Additionally, the rheobase was notably decreased in the fasted cohort compared to the *ad libitum*-fed cohort. Interestingly, N/OFQ^{ARC} neurones recorded from acute HFD-fed mice displayed a significant decrease in threshold current and a significantly greater number of action potentials (Jais et al., 2020), as we show currently in N/OFQ^{ARC} neurones recorded from fasted animals. This hyperexcitability of N/OFQ^{ARC} neurones may increase the incidence of phasic burst firing patterns in these cells. These observations fall in line with previous studies (Amini et al., 1999; Cain & Snutch, 2013) which describe that neuronal populations such as dopamine neurones in the midbrain display a lower threshold for activation, and oscillatory burst firing patterns that are calcium dependent. We were able to successfully abolish the oscillatory phasic burst firing seen in N/OFQ^{ARC} neurones upon dialysis of the calcium chelator BAPTA into the cytoplasm of N/OFQ^{ARC} cells via BAPTA-containing electrodes. Thus, it follows that the hyperactivity of N/OFQ^{ARC} neurones under conditions of negative (or positive) energy balance further promotes the release of endogenous N/OFQ peptide.

Stimulation of N/OFQ^{ARC} neurones inhibits POMC^{ARC} neurones to a greater degree under fasted conditions

Previous research in our lab has depicted that activation of NOP receptors inhibited neurotransmission at the N/OFQ^{ARC}/POMC^{ARC} and N/OFQ^{VTA}/A_{10} dopamine synapses (Hernandez et al., 2021). Additionally, exogenous application of N/OFQ inhibited POMC^{ARC} neurones as depicted by a reversible outward current, accompanied by a change in conductance that resulted in POMC hyperpolarization and decreased firing. Conditions of positive energy balance, such as DIO, promoted greater inhibitory effects of N/OFQ in POMC^{ARC} neurones (Hernandez et al., 2019). Similarly, on the opposing end of the energy balance spectrum, we also found that stimulation of the NOP receptor via endogenously released N/OFQ elicited by chemogenetic or optogenetic stimulation of N/OFQ^{ARC} neurones promoted a greater inhibitory effect on POMC^{ARC} neurones. We found that under fasted conditions, N/OFQ^{ARC} neurones produced a greater reversible inhibitory outward current and change in conductance in POMC^{ARC} neurones compared to cells from sated, *ad libitum*-fed controls.

The outward current in POMC^{ARC} neurones was elicited by N/OFQ–NOP receptor activation of GIRK channels. This is evidenced by the reversal potential of approximately −90 mV (very near the Nernst equilibrium potential for K^+) in both the fasted and *ad libitum*-fed groups, as well as by the increase in slope conductance, effects that are blocked by GIRK channel blockers like

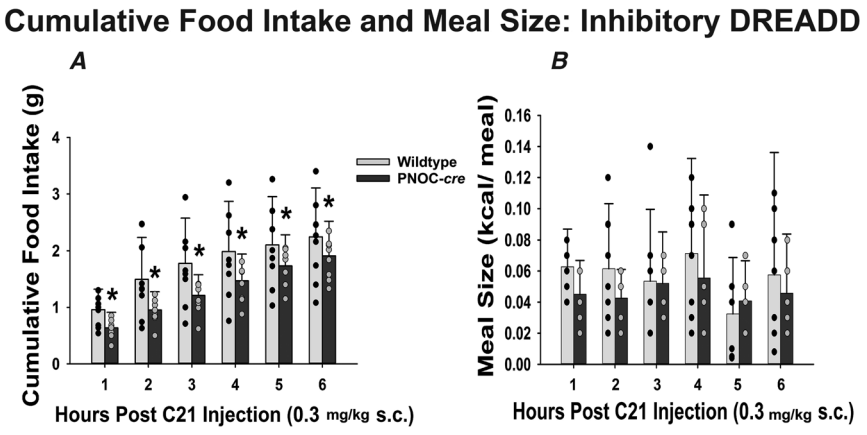

Figure 10. Cre-dependent chemoinhibition of N/OFQ^{ARC} neurones blunts the sustained rebound hyperphagia seen upon re-feeding following a fast
A, composite data depicting C21 promotes a significant decrease in cumulative food intake across the 6 h re-feed period. $^*P < 0.05$, relative to wild-type. *B*, composite data illustrating chemoinhibition of N/OFQ^{ARC} neurones promotes modest but not statistically significant decrease in meal size. $^*P < 0.05$, relative to wild-type; wild-type $n = 8$ animals; PNOC-*cre* $n = 8$ animals.

Ba^{2+} and tertiapin (Borgquist et al., 2013; Farhang et al., 2010; Wagner et al., 1998). The change in slope conductance occurred at a greater rate in the fasted group as opposed to the *ad libitum* group, corresponding with the greater inhibitory outward current seen in the fasted group compared to the *ad libitum* group upon stimulation of N/OFQ^{ARC} neurones. Additionally, activation of NOP receptors are implicated in inhibition of other brain regions such as the locus coeruleus where N/OFQ activated potassium channels (Connor et al., 1996). Within the dorsal raphe, NOP receptor-mediated inhibition of 5HT neurones occurs via activation of GIRK channels (Nazzaro et al., 2010). Moreover, N/OFQ inhibits SF-1/PACAP neurones in the VMN (Hernandez et al., 2019), melanin concentrating hormone neurones in the suprachiasmatic nucleus (Parsons & Hirasawa, 2011), and neurones in the periaqueductal grey (Vaughan et al., 1997). This evidence supports the notion that the inhibitory outward current seen in $POMC^{ARC}$ neurones is the result of NOP receptor activation of GIRK channels, promoting potassium efflux and membrane hyperpolarization.

E_2 attenuates the robust N/OFQ^{ARC} neurone-induced inhibition of $POMC^{ARC}$ neurones

Previously, our lab has reported that N/OFQ–NOP receptor activation of GIRK channels is physiologically antagonized by E_2 (Borgquist et al., 2013, 2014; Conde et al., 2016; Hernandez et al., 2019, 2021). We found in the present study, that although the inhibitory input from N/OFQ^{ARC} neurones onto $POMC^{ARC}$ neurones is potentiated under negative energy balance, this effect is greatly attenuated in the presence of E_2. Stimulation of endogenous N/OFQ release in the absence of E_2 elicited a robust outward current in $POMC^{ARC}$ neurones from OVX female animals. This robust inhibitory effect was also seen in $POMC^{ARC}$ neurones from intact males. However, we saw a striking difference in the inhibitory response of $POMC^{ARC}$ neurones during recordings in E_2-treated slices from OVX females. The presence of E_2 significantly decreased the change in current and conductance, rendering the $POMC^{ARC}$ neurones less inhibited, and promoting the anorexigenic signalling. N/OFQ is capable of hyperpolarizing both $SF\text{-}1/PACAP^{VMN}$ neurones and $POMC^{ARC}$ neurones, as well as diminishing $SF\text{-}1/PACAP^{VMN}$ glutamate release at synapses formed between the two cell types (Hernandez et al., 2019). The attenuating effects of E_2 are mediated via activation of ERα and Gq-mER. ERα and Gq-mER facilitate the uncoupling of $G_{i/o}$ receptors, and PI3K, PLC, PKC, and PKA signalling molecules transduce the uncoupling of NOP receptors and GIRK channels. This uncoupling is initiated upon E_2 binding to ERα or Gq-mER. For Gq-mER-mediated signalling PKC, activated by diacylglycerol, is upstream of PKA, phosphorylates adenylyl cyclase, which leads to the conversion of ATP to cyclic adenosine monophosphate (cAMP). cAMP activates PKA downstream, which phosphorylates either the GIRK channel or the NOP receptor. For ERα-mediated signalling, PI3K phosphorylates nNOS, and the nitric oxide thus formed can conceivably trigger receptor–effector uncoupling through protein nitrosylation (Conde et al., 2016). Given that both $SF\text{-}1/PACAP^{VMN}$ and $POMC^{ARC}$ neurones are responsive to E_2, the presence of E_2 uncouples the NOP receptor from the GIRK channels in these neuronal populations. The E_2-mediated NOP receptor uncoupling from GIRK channels restores the synaptic transmission between the $SF\text{-}1/PACAP^{VMN}/POMC^{ARC}$ neurones, and therefore promotes anorexigenic signalling in the ARC via α-melanocyte-stimulating-hormone release from $POMC^{ARC}$ neurones, and promotion of anorexigenic signals in the PVN to promote satiation and modulation of feeding behaviour. These modulatory processes at work in the oestrogenic regulation of appetite occur in both males and females (Smith et al., 2013).

E_2 has been shown to attenuate orexigenic signals by dampening cannabinoid sensitivity and attenuating cannabinoid 1 receptor (CB1R) presynaptic inhibition of glutamatergic input onto $POMC^{ARC}$ neurones, as well as impairing the NOP and μ-opioid receptor-mediated activation of GIRK channels in $POMC^{ARC}$ neurones in OVX female rats subjected to E_2 (Borgquist et al., 2015; Kellert et al., 2009; Kelly et al., 2002; Lagrange et al., 1994, 1997; Mela et al., 2016). GIRK channels have been shown to profoundly influence the excitability of $POMC^{ARC}$ neurones. Activation of GIRK channels leads to potassium efflux and hyperpolarization of resting membrane potential (RMP), which consequently inhibits the ability of $POMC^{ARC}$ neurones to generate action potentials (Kelly et al., 1990). E_2 increases neuronal excitability via desensitizing, or uncoupling, metabotropic $G_{i/o}$ receptors from GIRK channels (Borgquist et al., 2013; Kelly et al., 2002; Lagrange et al., 1994, 1997; Malyala et al., 2008). Taking this information into consideration, along with previous research demonstrating the ability of E_2 to attenuate the inhibitory effects of $G_{i/o}$ GPCRs, it is justified to draw the conclusion that $POMC^{ARC}$ neurones are influenced by the presence of E_2.

Hyperexcitability of N/OFQ^{ARC} neurones elicits a greater endogenous inhibitory tone in $POMC^{ARC}$ neurones

Utilizing pharmacological and chemoinhibitory means (i.e. the NOP receptor peptide antagonist UFP-101 and hM4D(Gi) DREADD, respectively), we found that the

disinhibition of POMC^{ARC} neurones was greatest in recordings taken from fasted conditions as opposed to *ad libitum* conditions. These results support our previous data collected from this study indicating that negative energy balance promotes hyperexcitability of N/OFQ^{ARC} neurones and potentiates the inhibitory effects onto POMC^{ARC} neurones. Consistent with our findings, I.C.V. administration of UFP-101 (3.7 or 7.4 nmol/rat) prior to N/OFQ (1.68 nmol/rat) completely abolished the hyperphagic effect elicited by N/OFQ (Economidou et al., 2006). Although the sample size was less than ideal, our results suggested that chemoinhibition of N/OFQ^{ARC} neurones also disrupted N/OFQ–NOP receptor signalling in a manner similar to that seen pharmacologically. Along these lines, chemoinhibition of N/OFQ^{VTA} neurones successfully prevented N/OFQ–NOP receptor signalling as evidenced by increased nose-pokes and number of sucrose rewards (Parker et al., 2019). This increased motivation for reward was achieved by the chemoinhibition of N/OFQ^{VTA} neurones (Parker et al., 2019) and therefore increased dopamine release promoting the motivation for reward (Olianas et al., 2008). Similarly, we found that optogenetic stimulation of N/OFQ^{VTA} neurones produced a robust outward current in A_{10} dopamine neurones, and intra-VTA N/OFQ diminished binge-like consumption *in vivo* (Hernandez et al., 2021). Therefore, it is evident that the pharmacological and chemoinhibitory means utilized in our experiments were successful in abrogating N/OFQ–NOP receptor signalling, leading to disinhibition of POMC^{ARC} neurones by removing the N/OFQ-induced inhibition of these cells, which occurs to a greater extent under condition of negative energy balance.

In vivo intra-ARC administration of N/OFQ and chemoexcitation of N/OFQ^{ARC} neurones augments the rebound hyperphagia during the re-feed following a fast in an E_2-dependent manner

The ARC has been depicted to be the most sensitive site in the elicitation of N/OFQ-induced hyperphagia, more so than any other hypothalamic region (Polidori et al., 2000). This is evidenced by the fact that intra-ARC injections of N/OFQ (0.21 or 0.42 nmol) elicited a significant increase in food intake 60 min post-injection in freely feeding rats, whereas administration into the VMN, PVN or the amygdala was without effect (Polidori et al., 2000). Our findings illustrate that the intra-ARC injection of N/OFQ promotes rebound hyperphagia characterized by significant elevations in cumulative food intake and increased meal size measured over 6 h following an 18-h period of fasting. These results indicate that although there were no differences in cumulative food intake during the first 2 h, the exogenous application of N/OFQ continually promoted appetitive behaviour during the mid to latter stages of the re-feed period. Additionally, exogenous application of N/OFQ promoted an overall increase in meal size compared to saline-treated counterparts. These results were shown to be sexually disparate, with the presence of EB attenuating the hyperphagic effects elicited by N/OFQ administration in OVX females. These effects of exogenously administered N/OFQ were replicated by *in vivo* chemogenetic excitation of N/OFQ^{ARC} neurones, which elicited robust increases in cumulative energy intake and meal size during the re-feed period. Conversely, chemoinhibition of these cells blunted the rebound hyperphagia seen upon re-feeding. These latter findings are in keeping with recent reports demonstrating successful employment of this approach, in which chemoexcitation of N/OFQ^{VTA} neurones promoted avoidance and decreased motivation for rewards in behavioural assays, and chemoinhibition of these cells did just the opposite (Parker et al., 2019).

Fasting brings about considerable neuronal plasticity in POMC neurones. Food-restricted animals displayed a decrease in POMC mRNA expression in the ARC, and corresponding with our results, food-restricted mice displayed robust rebound hyperphagia following a fast, as well as decreased plasma leptin levels (Lauzurica et al., 2010). In *ob*/ob mice lacking leptin, there is an increased number of excitatory inputs on NPY/AgRP^{ARC} neurones, a decreased number of excitatory synapses on POMC^{ARC} neurones, and correspondingly a greater number of spontaneous excitatory postsynaptic currents (sEPSCs) onto NPY neurones and a significantly greater degree of inhibitory input onto POMC^{ARC} neurones (Pinto et al., 2004). Similarly, in DIO OVX female guinea pigs and Nr5a1-*cre* mice (*Nr5a1* is the gene encoding steroidogenic factor-1 (SF-1)), there is a conspicuous lack of excitatory glutamatergic input onto POMC^{ARC} neurones emanating from SF-1^{VMN} neurones (Fabelo et al., 2018). Severe food restriction has been shown to stimulate the hypothalamic–pituitary–adrenal (HPA) axis (Akana et al., 1994). Fasting-induced hypoglycaemia is one of the most potent stressors, and the N/OFQ–NOP system is clearly important in coping with this stress as NOP receptor deficient mice exhibit a muted rebound hyperphagic response during the re-feed period. NOP receptor knockout mice displayed reduced food intake during the 6 h re-feed period following a fast and reduced meal duration frequency and size (Farhang et al., 2010). This, coupled with the results of the present study, strongly indicates that N/OFQ^{ARC} neurones play a vital role in mitigating the adverse impact of negative energy balance by inhibiting anorexigenic neural substrates and heightening appetitive behaviour.

Taken together, these results indicate negative energy balance induces hyperactivity of N/OFQ^{ARC} neurones, and this hyperactivity elicits greater inhibitory effects

onto $POMC^{ARC}$ neurones. These inhibitory effects are attributed to NOP receptor activation of GIRK channels, ultimately hyperpolarizing $POMC^{ARC}$ neurones, and a sustained hyperphagic response *in vivo*. However, the magnitude of these inhibitory effects is markedly attenuated in the presence of E_2. These results lend insight to the pathoneurological mechanisms underlying metabolic disorders, and provide insight as to why those lacking E_2 are more susceptible to such disorders.

References

Akana, S. F., Strack, A. M., Hanson, E. S., & Dallman, M. F. (1994). Regulation of activity in the hypothalamo-pituitary-adrenal axis is integral to a larger hypothalamic system that determines caloric flow. *Endocrinology*, **135**(3), 1125–1134.

Amini, B., Clark, J. W., Jr., & Canavier, C. C. (1999). Calcium dynamics underlying pacemaker-like and burst firing oscillations in midbrain dopaminergic neurons: A computational study. *Journal of Neurophysiology*, **82**(5), 2249–2261.

Andrews, W. W., Advis, J. P., & Ojeda, S. R. (1981). The maturation of estradiol-negative feedback in female rats: Evidence that the resetting of the hypothalamus "gonadostat" does not precede the first preovulatory surge of gonadotropins. *Endocrinology*, **109**(6), 2022–2031.

Bewick, G. A., Dhillo, W. S., Darch, S. J., Murphy, K. G., Gardiner, J. V., Jethwa, P. H., Kong, W. M., Ghatei, M. A., & Bloom, S. R. (2005). Hypothalamic cocaine- and amphetamine-regulated transcript (CART) and agouti-related protein (AgRP) neurons coexpress the NOP1 receptor and nociceptin alters CART and AgRP release. *Endocrinology*, **146**(8), 3526–3534.

Borgquist, A., Kachani, M., Tavitian, N., Sinchak, K., & Wagner, E. J. (2013). Estradiol negatively modulates the pleiotropic actions of orphanin FQ/nociceptin at proopiomelanocortin synapses. *Neuroendocrinology*, **98**(1), 60–72.

Borgquist, A., Meza, C., & Wagner, E. J. (2015). Role of neuronal nitric oxide synthase in the estrogenic attenuation of cannabinoid-induced changes in energy homeostasis. *Journal of Neurophysiology*, **113**(3), 904–914.

Borgquist, A., Rivas, V. M., Kachani, M., Sinchak, K., & Wagner, E. J. (2014). Gonadal steroids differentially modulate the actions of orphanin FQ/nociceptin at a physiologically relevant circuit controlling female sexual receptivity. *Journal of Neuroendocrinology*, **26**(5), 329–340.

Bunzow, J. R., Saez, C., Mortrud, M., Bouvier, C., Williams, J. T., Low, M., & Grandy, D. K. (1994). Molecular cloning and tissue distribution of a putative member of the rat opioid receptor gene family that is not a μ, δ or kappa opioid receptor type. *FEBS Letters*, **347**(2–3), 284–288.

Cain, S. M., & Snutch, T. P. (2013). T-type calcium channels in burst-firing, network synchrony, and epilepsy. *Biochimica et Biophysica Acta*, **1828**(7), 1572–1578.

Chang, R., Hernandez, J., Gastelum, C., Guadagno, K., Perez, L., & Wagner, E. J. (2021). Pituitary adenylate cyclase-activating polypeptide excites proopiomelanocortin neurons: implications for the regulation of energy homeostasis. *Neuroendocrinology*, **111**(1–2), 45–69.

Chee, M. J., Price, C. J., Statnick, M. A., & Colmers, W. F. (2011). Nociceptin/orphanin FQ suppresses the excitability of neurons in the ventromedial nucleus of the hypothalamus. *Journal of Physiology*, **589**(13), 3103–3114.

Conde, K., Fabelo, C., Krause, W. C., Propst, R., Goethel, J., Fischer, D., Hur, J., Meza, C., Ingraham, H. A., & Wagner, E. J. (2017). Testosterone rapidly augments retrograde endocannabinoid signaling in proopiomelanocortin neurons to suppress glutamatergic input from steroidogenic factor 1 neurons via upregulation of diacylglycerol lipase-α. *Neuroendocrinology*, **105**(4), 341–356.

Conde, K., Meza, C., Kelly, M. J., Sinchak, K., & Wagner, E. J. (2016). Estradiol rapidly attenuates ORL-1 receptor-mediated inhibition of proopiomelanocortin neurons via G_q-coupled, membrane-initiated signaling. *Neuroendocrinology*, **103**(6), 787–805.

Connor, M., Vaughan, C. W., Chieng, B., & Christie, M. J. (1996). Nociceptin receptor coupling to a potassium conductance in rat locus coeruleus neurones *in vitro*. *British Journal of Pharmacology*, **119**(8), 1614–1618.

Economidou, D., Policani, F., Angellotti, T., Massi, M., Terada, T., & Ciccocioppo, R. (2006). Effect of novel NOP receptor ligands in food intake in rats. *Peptides*, **27**(4), 775–783.

Emmerson, P. J., & Miller, R. J. (1999). Pre- and postsynaptic actions of opioid and orphan opioid agonists in the rat arcuate nucleus and ventromedial hypothalamus *in vitro*. *Journal of Physiology*, **517**(2), 431–445.

Fabelo, C., Hernandez, J., Chang, R., S, S., Alicea, N., Tian, S., Conde, K., & Wagner, E. J. (2018). Endocannabinoid signaling at hypothalamic steroidogenic factor-1/proopiomelanocortin synapses is sex- and diet-sensitive. *Frontiers in Molecular Neuroscience*, **11**, 214.

Farhang, B., Pietruszewski, L., Lutfy, K., & Wagner, E. J. (2010). The role of the NOP receptor in regulating food intake, meal pattern, and the excitability of proopiomelanocortin neurons. *Neuropharmacology*, **59**(3), 190–200.

Gallo, R. V., & Bona-Gallo, A. (1985). Lack of ovarian steroid negative feedback on pulsatile luteinizing hormone release between estrus and diestrus day 1 in the rat estrous cycle. *Endocrinology*, **116**(4), 1525–1528.

Gomez, J. L., Bonaventura, J., Lesniak, W., Mathews, W. B., Sysa-Shah, P., Rodrieguez, L. A., Ellis, R. J., Richie, W. B., Harvey, B. K., Dannals, R. F., Pomper, M. G., Bonci, A., & Michaelides, M. (2017). Chemogenetics revealed: DREADD occupancy and activation via converted clozapine. *Science*, **357**(6350), 503–507.

Hernandez, J., Fabelo, C., Perez, L., Moore, C., Chang, R., & Wagner, E. J. (2019). Nociceptin/orphanin FQ modulates energy homeostasis through inhibition of neurotransmission at VMN SF-1/ARC POMC synapses in a sex- and diet-dependent manner. *Biology of Sex Differences*, **10**, https://doi.org/10.1186/s13293-13019-10220-13293.

Hernandez, J., Perez, L., Soto, R., Le, N., Gastelum, C., & Wagner, E. J. (2021). Nociceptin/orphanin FQ neurons in the arcuate nucleus and ventral tegmental area act via nociceptin opioid peptide receptor signaling to inhibit proopiomelanocortin and a 10 dopamine neurons and thereby modulate ingestion of palatable food. *Physiology & Behavior*, **228**, 113183.

Inui, A. (2002). Cancer anorexia-cachexia syndrome: Current issues in research and management. *CA*, **52**(2), 72–91.

Jais, A., Paeger, L., Sotelo-Hitschfeld, T., Bremser, S., Prinzensteiner, M., Klemm, P., Mykytiuk, V., Widdershooven, P. J. M., Vesting, A. J., Grzelka, K., Minere, M., Cremer, A. L., Xu, J., Korotkova, T., Lowell, B. B., Zeilhofer, H. U., Backes, H., Fenselau, H., Wunderlich, F. T., Kloppenburg, P., & Brüning, J. C. (2020). PNOC^{ARC} neurons promote hyperphagia and obesity upon high-fat feeding. *Neuron*, **106**(6), 1009–1025.e10.

Kellert, B. A., Nguyen, M. C., Nguyen, C., Nguyen, Q. H., & Wagner, E. J. (2009). Estrogen rapidly attenuates cannabinoid-induced changes in energy homeostasis. *European Journal of Pharmacology*, **622**(1–3), 15–24.

Kelly, M. J., Loose, M. D., & Ronnekleiv, O. K. (1990). Opioids hyperpolarize β-endorphin neurons via μ-receptor activation of a potassium conductance. *Neuroendocrinology*, **52**(3), 268–275.

Kelly, M. J., Rønnekleiv, O. K., Ibrahim, N., Lagrange, A. H., & Wagner, E. J. (2002). Estrogen modulation of K^+ channel activity in hypothalamic neurons involved in the control of the reproductive axis. *Steroids*, **67**(6), 447–456.

Kelly, M. J., & Wagner, E. J. (1999). Estrogen modulation of G-protein-coupled receptors. *Trends in Endocrinology and Metabolism*, **10**(9), 369–374.

Kotz, C. M., Briggs, J. E., Grace, M. K., Levine, A. S., & Billington, C. J. (1998). Divergence of the feeding and thermogenic pathways influenced by NPY in the hypothalamic PVN of the rat. *American Journal of Physiology*, **275**, R471-477.

Lagrange, A. H., Ronnekleiv, O. K., & Kelly, M. J. (1994). The potency of μ-opioid hyperpolarization of hypothalamic arcuate neurons is rapidly attenuated by 17β-estradiol. *Journal of Neuroscience*, **14**(10), 6196–6204.

Lagrange, A. H., Ronnekleiv, O. K., & Kelly, M. J. (1997). Modulation of G protein-coupled receptors by an estrogen receptor that activates protein kinase A. *Molecular Pharmacology*, **51**(4), 605–612.

Lauzurica, N., García-García, L., Pinto, S., Fuentes, J. A., & Delgado, M. (2010). Changes in NPY and POMC, but not serotonin transporter, following a restricted feeding/repletion protocol in rats. *Brain Research*, **1313**, 103–112.

Le, N., Hernandez, J., Gastelum, C., Perez, L., Vahrson, I., Sayers, S., & Wagner, E. J. (2021). Pituitary adenylate cyclase activating polypeptide inhibits A(10) dopamine neurons and suppresses the binge-like consumption of palatable food. *Neuroscience*, **478**, 49–64.

Malyala, A., Zhang, C., Bryant, D. N., Kelly, M. J., & Rønnekleiv, O. K. (2008). PI3K signaling effects in hypothalamic neurons mediated by estrogen. *Journal of Comparative Neurology*, **506**(6), 895–911.

Matsushita, H., Ishihara, A., Mashiko, S., Tanaka, T., Kanno, T., Iwaasa, H., Ohta, H., & Kanatani, A. (2009). Chronic intracerebroventricular infusion of nociceptin/orphanin FQ produces body weight gain by affecting both feeding and energy metabolism. *Endocrinology*, **150**(6), 2668–2673.

Mattis, J., Tye, K. M., Ferenczi, E. A., Ramakrishnan, C., O'Shea, D. J., Prakash, R., Gunaydin, L. A., Hyun, M., Fenno, L. E., Gradinaru, V., O, Y., & Deisseroth, K. (2012). Principles for applying optogenetic tools derived from direct comparitive analysis of microbial opsins. *Nature Methods*, **9**(2), 159–172.

Meis, S., & Pape, H.-C. (2001). Control of glutamate and GABA release by nociceptin/orphanin FQ in the rat lateral amygdala. *Journal of Physiology*, **532**(3), 701–712.

Mela, V., Vargas, A., Meza, C., Kachani, M., & Wagner, E. J. (2016). Modulatory influences of estradiol and other anorexigenic hormones on metabotropic, Gi/o-coupled receptor function in the hypothalamic control of energy homeostasis. *Journal of Steroid Biochemistry and Molecular Biology*, **160**, 15–26.

Meunier, J.-C. (1997). Nociceptin/orphanin FQ and the opioid receptor-like ORL_1 receptor. *European Journal of Pharmacology*, **340**(1), 1–15.

Nazzaro, C., Barbieri, M., Varani, K., Beani, L., Valentino, R. J., & Siniscalchi, A. (2010). Swim stress enhances nociceptin/orphanin FQ-induced inhibition of rat dorsal raphe nucleus activity in vivo and in vitro: Role of corticotropin releasing factor. *Neuropharmacology*, **58**(2), 457–464.

Olianas, M. C., Dedoni, S., Boi, M., & Onali, P. (2008). Activation of nociceptin/orphanin FQ-NOP receptor system inhibits tyrosine hydroxylase phosphorylation, dopamine synthesis, and dopamine D(1) receptor signaling in rat nucleus accumbens and dorsal striatum. *Journal of Neurochemistry*, **107**(2), 544–556.

Olszewski, P. K., & Levine, A. S. (2004). Minireview: characterization of influence of central nociceptin/orphanin FQ on consummatory behavior. *Endocrinology*, **145**(6), 2627–2632.

Parker, K. E., Pedersen, C. E., Gomez, A. M., Spangler, S. M., Walicki, M. C., Feng, S. Y., Stewart, S. L., Otis, J. M., Al-Hasani, R., McCall, J. G., Sakers, K., Bhatti, D. L., Copits, B. A., Gereau, R. W., Jhou, T., Kash, T. J., Dougherty, J. D., Stuber, G. D., & Bruchas M. R. (2019). A paranigral VTA nociceptin circuit that constrains motivation for reward. *Cell*, **178**(3), 653–671.e19.

Parsons, M. P., & Hirasawa, M. (2011). GIRK channel-mediated inhibition of melanin-concentrating hormone neurons by nociceptin/orphanin FQ. *Journal of Neurophysiology*, **105**(3), 1179–1184.

Pinto, S., Roseberry, A. G., Liu, H., Diano, S., Shanabrough, M., Cai, X., Friedman, J. M., & Horvath, T. L. (2004). Rapid rewiring of arcuate nucleus feeding circuits by leptin. *Science*, **304**(5667), 110–115.

Polidori, C., de Caro, G., & Massi, M. (2000). The hyperphagic effect of nociceptin/orphanin FQ in rats. *Peptides*, **21**(7), 1051–1062.

Pomonis, J. D., Billington, C. J., & Levine, A. S. (1996). Orphanin FQ, agonist of the orphan opioid receptor, stimulates feeding in rats. *Neuroreport*, **8**(1), 369–371.

Qiu, J., Bosch, M. A., Tobias, S. C., Krust, A., Graham, S. M., Murphy, S. J., Korach, K. S., Chambon, P., Scanlan, T. S., Rønnekleiv, O. K., & Kelly, M. J. (2006). A g-protein-coupled estrogen receptor is involved in hypothalamic control of energy homeostasis. *Journal of Neuroscience*, **26**(21), 5649–5655.

Qiu, J., Nestor, C. C., Zhang, C., Padilla, S. L., Palmiter, R. D., Kelly, M. J., & Ronnekleiv, O. K. (2016). High-frequency stimulation-induced peptide release synchronizes arcuate kisspeptin neurons and excites GnRH neurons. *eLife*, **5**, e16246.

Riggs, P. K., Vaida, F., Rossi, S. S., Sorkin, L. S., Gouaux, B., Grant, I., & Ellis, R. J. (2012). A pilot study of the effects of cannabis on appetite hormones in HIV-infected adult men. *Brain Research*, **1431**, 46–52.

Saper, C. B., Chou, T. C., & Elmquist, J. K. (2002). The need to feed: homeostatic and hedonic control of eating. *Neuron*, **36**(2), 199–211.

Sinchak, K., Romeo, H. E., & Micevych, P. E. (2006). Site-specific estrogen and progestin regulation of orphanin FQ/nociceptin and nociceptin opioid receptor mRNA expression in the female rat limbic hypothalamic system. *Journal of Comparative Neurology*, **496**(2), 252–268.

Smith, A. W., Bosch, M. A., Wagner, E. J., Rønnekleiv, O. K., & Kelly, M. J. (2013). The membrane estrogen receptor ligand STX rapidly enhances GABAergic signaling in NPY/AgRP neurons: role in mediating the anorexigenic effects of 17β-estradiol. *American Journal of Physiology. Endocrinology and Metabolism*, **305**(5), E632-E640.

Stratford, T. R., Holahan, M. R., & Kelley, A. E. (1997). Injections of nociceptin into the nucleus accumbens shell or ventromedial hypothalamic nucleus increase food intake. *Neuroreport*, **8**(2), 423–426.

Vaughan, C. W., Ingram, S. L., & Christie, M. J. (1997). Actions of the ORL_1 receptor ligand nociceptin on membrane properties of rat periaqueductal gray neurons *in vitro*. *Journal of Neuroscience*, **17**(3), 996–1003.

Wagner, E. J., Rønnekleiv, O. K., Grandy, D. K., & Kelly, M. J. (1998). The peptide orphanin FQ inhibits β-endorphin neurons and neurosecretory cells in the hypothalamic arcuate nucleus by activating an inwardly-rectifying K^+ conductance. *Neuroendocrinology*, **67**(1), 73–82.

Zigman, J. M., & Elmquist, J. K. (2003). Minireview: From anorexia to obesity–the yin and yang of body weight control. *Endocrinology*, **144**(9), 3749–3756.

Additional information

Competing interests

None.

Author contributions

S.S., N.L. and J.H., performed all stereotaxic and survival surgeries. S.S. and J.H. performed all electrophysiological recordings. S.S., N.L., J.H. and V.M.P., performed all metabolic studies. S.S. and E.J.W. performed data analysis for all electrophysiology and metabolic studies. S.S. and E.J.W. created all figures and performed statistical analysis. S.S. and E.J.W generated the manuscript, and all authors edited the final manuscript. E.J.W. and S.S. designed the experiments. All authors have read and approved the final version of this manuscript and agree to be accountable for all aspects of the work in ensuring that questions related to the accuracy or integrity of any part of the work are appropriately investigated and resolved. All persons designated as authors qualify for authorship, and all those who qualify for authorship are listed.

Funding

This work was supported by PHS Grant DA024314 and intramural funding from Western University of Health Sciences.

Data availability statement

All the data supporting our interpretations and conclusions have been included in the Results section of the manuscript.

Keywords

energy balance, fasting, nociceptin/orphanin FQ, proopiomelanocortin, oestradiol, sex differences

Supporting information

Additional supporting information can be found online in the Supporting Information section at the end of the HTML view of the article. Supporting information files available:

Statistical Summary Document
Peer Review History